SCAVENGING EFFECTS OF DIETARY FLAVONOIDS ON REACTIVE DICARONYL SPECIES AND THEIR POSSIBLE IMPLICATIONS ON THE INHIBITION OF THE FORMATION OF ADVANCED GLYCATION-END PRODUCTS

by

XI SHAO

A dissertation submitted to the

Graduate School-New Brunswick

Rutgers, The State University of New Jersey

in partial fulfillment of the requirements

for the Degree of

Doctor of Philosophy

Graduate Program in Food Science

Written under the direction of

Professors Shengmin Sang & Chi-Tang Ho

and approved by

_____

_____

_____

_____

New Brunswick, New Jersey

October, 2010

ABSTRACT OF THE DISSERTATION

SCAVENGING EFFECTS OF REACTIVE DICARONYL SPECIES BY DIETARY FLAVONOIDS AND THEIR POSSIBLE IMPLICATIONS ON THE INHIBITION OF THE FORMATION OF ADVANCED GLYCATION-END PRODUCTS

BY XI SHAO

Dissertation Director: Professors Shengmin Sang & Chi-Tang Ho

Flavonoids are ubiquitous in nature and many of which occur in fruits, vegetables and beverages. According to chemical structure, flavonoids can be categorized into flavonols, flavones, flavanones, isoflavones, flavanols, anthocyanidins and chalcones. The flavonoids have aroused considerable interest recently because of their potential health benefits. They have been reported to reduce the risk of cancer, cardiovascular diseases, asthma, and diabetes. The objects of this study are to elucidate the structure-activity of dietary flavonoids to trap dicarbonyl species (e.g., glyoxal (GO) and methylglyoxal (MGO)), which are the precursors of advanced glycation end products (AGEs), as well as to study the possible implications on the inhibition of the formation of AGEs by flavonoids. Previous studies have demonstrated that accumulation of reactive dicarbonyl compounds in human tissue will accelerate the vascular damage in both diabetes and uremia. Moreover, advanced glycation progressively and irreversibly modified proteins over time and yielded AGEs. AGEs are thought to contribute to the development of diabetes mellitus and its complications. Higher levels of α, β-dicarbonyl compounds were observed in diabetes patients' plasma than those in healthy people's plasma. Therefore, decreasing the levels of dicarbonyl compounds and consequently inhibiting the formation of AGEs would be a useful approach to prevent the development of diabetic complications.

In this dissertation, we found that polyphenols phloretin and phloridzin from could trap MGO rapidly under *in vitro* conditions (pH 7.4 buffer solution, 37 ^{o}C) to form carbonyl adducts of those two compounds. The mono-carbonyl adduct of phloridzin was purified through column chromatography and identified by ^{1}H, ^{13}C, and 2D NMR and MS analysis.

To understand the structure requirements of flavonoids to perform good trapping effects of reactive dicarbonyl compounds, we tested the trapping efficacy of flavonoids with different A-ring, B-ring, and C-ring configuration under *in vitro* conditions. Genistein, phloretin, and phloridzin were tested under an AGEs condition and all three flavonoids exhibited strong inhibitory effects on the formation AGEs. Two reaction adducts of genistein under such condition were observed using LC/MS, which further confirmed that flavonoids have the ability to prevent the formation of AGEs through trapping of dicarbonyl species.

ACKNOWLEDGEMENTS

I would like to take this opportunity to thank Dr. Shengmin Sang and Dr. Chi-Tang Ho for their mentoring, continuous encouragement and stimulating suggestions.

I would also like to thank my committee member, Dr. Chung S. Yang and Dr. M-T Huang, for their support and valuable suggestions. I thank Dr. Naisheng Bai for his help and suggestions for my career development. I appreciate Mr. Marlon Lee's technical instructions, Ms. Anna Liu, Miss. Tiffany Parks, and Ms. Dorothy Wong's warmhearted help during my stay in the lab. I benefited a lot from the discussion with Dr. Lishuang Lv.

Finally, I would like to express my deep appreciation to my families for their continuous encouragement and support. Without their generous love, I would not have had the opportunity for such a high value of education and working with so many great and nice people.

TABLE OF CONTENTS

LIST OF TABLES AND ILLUSTRATIONS

LIST of ABBREVIATION

AGEs	advanced glycation end products
BSA	bovine serum albumin
CEL	carboxyethyllysine
CML	carboxymethyllysine
CPC	conventional polyclonal anti-CML antibody
DAG	diacylglycerol
DHA-P	dihydroxyacetone phosphate
ECG	(-)-epicatechin gallate
EDC	electron capture detector
EGCG	(-)-epigallocatechin gallate
ELISA	enzyme linked immunosorbent assay
ESI/LC/MS	electrospray ionization liquid chromatography/mass spectrometry
F 1-6 DP	fructose 1,6- diphosphate
FN3K	fructosamine 3-kinase
GA3P	glyceraldehydes 3-phosphate
GC	gas chromatography
GO	glyoxal
GOLD	glyoxal-lysine dimmer
HPLC	high performance liquid chromatography
JNK	c-Jun N-terminal kinase
LDH	lactate dehydrogenase
LDL	low density lipoprotein

MAPK	mitogen activated protein kinase
MGO	methylglyoxal
MOLD	methylglyoxal-lysine dimmer
MS/SIM	mass spectrometry/selected ion monitor
NPD	nitrogen phosphorus detector
PCA	perchloric acid
PFBOA	pentafluorobenzyloxylamine
PK	pyruvate kinase
PKC	protein kinase C
ROS	reactive oxygen species
SPE	solid phase extraction
STZ	streptozocin
TFA	trifluroacetic acid
TRI	6-hydroxy-2, 4, 5-triaminopyrimidine
VSMCs	vascular smooth muscle cells

INTRODUCTION

1. Formation of reactive dicarbonyl compounds

The reactive dicarbonyl compounds, for example, MGO and GO, also named as α-Oxoaldehyde, α, β-diketone, have been widely concerned recently due to their highly reactive properties. They are readily form adducts with biological substances such as proteins, phospholipids, and DNA, thereby lead to the functional loss of these biological substances. Either the bioactive dicarbonyl compounds themselves or adducts generated by them result in several health issues, especially in relation to the complications of diabetes [1].

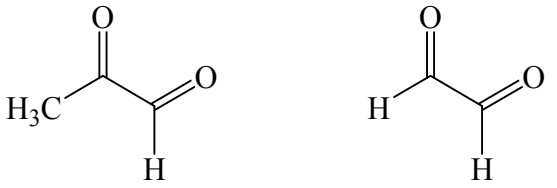

Methylglyoxal (MGO) Glyoxal (GO)

Figure 1. Chemical structures of MGO and GO

Generally, reactive dicarbonyl compounds exist in our daily food intakes as the exogenous sources, such as cookies, breads, coffee, honey, beverages, oils, water, and even cigarette smoke [2]. The endogenous reactive carbonyl compounds are produced through both enzymatic and nonenzymatic pathways.

1.1 Exogenous sources of MGO and GO

As the major precursor of MGO and GO, sugar contained food products and beverages represent most of the exogenous sources of these two dicarbonyl species. Such as cookie, oil, wine, beer, coffee, honey, coke. Moreover, MGO and GO also occur in water, rain, clouds, fog

water, and urban atmosphere and cigarette smoke. MGO and GO are formed by carbohydrate auto-oxidation and degradation, Maillard reaction, lipid peroxidation, and microorganisms during industrial processing, cooking, or prolonged storage.

1.1.1 MGO and GO in cookie and bread

As widely distributed foods in western diets, cookie and bread are two of the major exogenous sources of dicarbonyl compounds in our daily intake. Several studies have reported that the degradation of sugar moiety by retro-aldol condensation (Wolf pathway), auto-oxidation of carbohydrates and lipid peroxidation during thermal processing of cookies and breads lead the formation of dicarbonyl compounds.

MGO and GO as two major reactive dicarbonyl speices have been quantified in cookie and bread in several studies. The levels of MGO and GO were evaluated using chromatography method after the derivatization with 1, 2-diaminobenzene to produce stable quinoxaline derivatives. *Gema* and *Francisco* reported the value of MGO and GO in commercial cookies ranged from 3.7 to 81.4 mg/kg and 4.8 to 26.0 mg/kg, respectively [3]. In bread, MGO and GO were detected at a concentration of 0.30 ~ 0.79 mg/kg. In toasted bread, the levels of MGO and GO ranged from 0.5 to 2.5 mg/kg [4]. In *Poiter* and *Borovikova*'s study, GO was detected in bread crust and bread crumbs with a concentration of 1.6 mg/kg [5]. Moreover, *Gema* and *Francisco* have demonstrated that the formation of MGO and GO is associated with the baking time as the surface effect. As common ingredients in cookies, ammonium bicarbonate and fructose can facilitate the formation of dicarbonyl compounds by generating more MGO and GO comparing to the control group [6].

1.1.2 MGO and GO in beer and wine

Accumulation of MGO and GO occurs in the growth medium of microorganisms during many fermentation processes and matrixes, such as beer and wine. Dicarbonyl compounds in beer have drawn much attention recently due to both of the healthy concerns and the effects on beer flavor deteriorations. The formation of dicarbonyl compounds in beer occurs during the heating step of the brewing process through Maillard reaction and remained in the fresh and aged beer. MGO and GO are formed in different steps of the Maillard reaction. In early glycation, MGO and GO are generated from Schiff base through Namiki pathway. In advanced glycation, Amadori products induce the formation of MGO and GO through a serious complicated rearrangement. The reaction conditions, especially the temperature significantly influence the formation of MGO and GO in the Maillard reaction. For instance, the yields of MGO increased almost two folds when the temperature of reaction between glycine and β-alanine mixture increased from 100°C to 120°C. MGO as secondary dicarbonyl product was derived from the degradation of Amadori products compounds including 3-deoxy-2-hexosulose and 3-deoxy-2, 3-pentodiulose [7, 8].

The level of MGO as flavor precursors of beer was also detected using RP-HPLC after employing the derivatization strategy with 1, 2- diaminobenzene. In fresh and 1 week aged beer, the value of MGO is detected as 5.0 ± 0.1 μM and 5.0 ± 0.6 μM, respectively [9]. *Adriana* and *Rafael* also demonstrated that the level of MGO increases significantly during aging at a rate of 0.8 μM/week.

MGO and GO occur in all types of wine through synthesis by *Saccharomyces cerevisae* during alcoholic fermentation and also by *Oenococcus oerri* (*Leuconostoc oenos*) during malolactic fermentation. And the levels of dicarbonyls species vary a lot during alcoholic fermentation and malolactic fermentation, and ageing process [10]. *Gilles* and *Alain* reported the levels of MGO and GO ranged from 0.1 to 1.0 mg/L and 0.15 to 2.0 mg/L, respectively. A similar quantification method to determine the most abundant a-dicarbonyl compounds in wine using

HPLC was developed by reaction with 2, 3-diaminobenzene to form stable quinoxalines derivatives [11].

1.1.3 MGO and GO in coffee

MGO and GO are present in many foods and drinks, including coffee, the most popular drink in western world. Back to early 1980s, *Tateki* and *Takayuki* have reported trace amount of MGO in brew coffee, decaffeinate brew coffee, and instant coffee [12]. In a recent paper, it was reported that MGO and GO as Maillard reaction products in coffee extracts obtained from coffee beans with different degrees of roast [13].

Dicarbonyl species not only occur in roast coffee beans, small amounts of MGO and GO also found in green coffee beans. During roasting process, the levels of MGO and GO both increased, then declined. Thus, the highest values of MGO and GO are usually found in light and medium roasted coffees. In *Maria* and *Gabriella*'s study, coffee extracts firstly went through C18-SPE cartridge to eliminate interfering components. Then, dicarbonyl compounds reacted with 1, 2-diaminobenze to form quinoxaline derivatives. RP-HPLC-DAD was used for the quantification analysis. The concentration of MGO reached highest level at 21.19 ± 0.42 mg/100g after 10 min of roasting. The value of GO reached the peak concentration at 13.07 ± 0.39 mg/100g after 6 min of roasting. Both MGO and GO contents were decreased after reach their peak concentrations. This reduction phenomenon may be due to the involvement of MGO and GO in the advanced stages of Maillard reaction, which result in browning reaction (melanoidins).

1.1.4 MGO and GO in beverages

Due to high fructose corn syrup (HFCS) contents, carbonated soft drinks (CSD) are now considered as a potential source of dicarbonyl species. Conversion of glucose to fructose using

enzymatic manners was firstly developed by *Marshall* and *Kooi*, which is widely used in food and beverage industry as a liquid sweetener due to its low price and ease of handling [14].

Many studies have identified that dicarbonyl compounds usually occur during the glucose degradation and oxidation. CSD as a large consumed product over the world and high sugar-sweetened containing source have been screened for the possible presence of MGO and GO. In *Lo* and *Ho*'s recent studies, MGO and GO contents were analyzed in 13 CSDs. The derivatization reactions were performed using 1, 2-diaminobenzen for MGO and GO. Their corresponding quinoxaline analogues were further analyzed using HPLC-UV. MGO were found with a range of 7.1 ± 1.9 to 139.5 ± 2.1 μg/100 mL and the level of GO ranged from 2.0 ± 0.2 to 173.4 ± 2.8 μg/100 mL in 13 brands of CSD [15, 16]. To further verify the observations of dicarbonyls in CSD and their possible sources in drink, three HFCS samples were further tested to obtain the levels of MGO and GO in this study. Even the values of MGO and GO vary significantly from differentsources of HFCS due to different manufacturing processes and storage conditions, significantly high levels of MGO and GO were observed in these three HFCS samples. The concentrations of MGO and GO were ranged from 112.4 ± 0.1 to 385.1 ± 7.5 μg/100 mL and 18.1 ± 0.8 to 50.8 ± 0.2 μg/100 mL, respectively.

1.1.5 MGO and GO in honey

Honey as a system with high sugar content is prone to sugar degradation due to heating process applied during both manufacturing and storage. And sugar degradation in honey usually leads to the formation of dicarbonyl species through both caramelization and Maillard reaction.

In previous study, *Weigel et al*. have reported the amounts of the 1, 2-dicarbonyls; MGO and GO are present in 21 commercially available samples of honey. After derivatization with orthophenylenediamine (OPD), MGO and GO in honey were measured as the corresponding

quinoxalines using RP-HPLC. The concentrations of MGO and GO were ranged from 0.4 to 5.4 mg/kg and 0.2 to 2.7 mg/kg, respectively [17]. In a present study, The 1, 2-dicarbonyl compounds MGO and GO were measured as the corresponding quinoxalines after derivatization with orthophenylendiamine using RP-HPLC and UV-detection in 6 New Zealand Manuka (Leptospermum scoparium) honey samples. In which, MGO was found up to 100-folds higher than conventional honeys, ranging from 38 to 761 mg/kg. And the concentration of GO is ranged from 0.7 to 7.0 mg/kg, which was comparable to previously published data [18]. Results here indicated that the concentrations of MGO and GO in commercial honey products is not only associated with manufacturing and storage conditions, but also related to the origin of honeys.

1.1.6 MGO and GO in oil

The oxidative degradation of different lipids also leads to the formation of MGO and GO in food during storage or processing. Three mechanisms of lipid peroxidation were proposed so far: auto-oxidation by free radical reaction, photo-oxidation, and enzyme action. Besides the third one, reactive oxygen species (ROS), as initiators, play an important role in other two lipid peroxidation pathways [19].

Previous studies have demonstrated the formation of MGO and GO in different lipid origins: tuna, soybean, olive, and corn oils under accelerated storage (60°C for 3 and 7 days) or cooking (200°C for 1h) conditions. The highest concentration of GO was observed in salmon oil after heated at 60°C for 3 days. The values of GO found in salmon and cod liver oils when they were 12.8 ± 1.10 and 7.07 ± 0.19 ppm, respectively after heated for 3 days. Whereas, the amounts changed to 6.70 ± 0.08 and 5.94 ± 0.38 ppm, respectively after 7 days heating. The amount of MGO ranged from 2.03 ± 0.13 to 2.89 ± 0.11 ppm in the fish oils heated at 60°C for 7 days. Among vegetable oils, only olive oil form MGO (0.61 ± 0.03 ppm) under accelerated storage conditions [20]. The above results indicated that the formation of dicarbonyl compounds is

influenced by storage and cooking conditions. Moreover, the oils containing higher levels of long-chain PUFA, such as fish oils, produced more dicarbonyl compounds.

1.2 Endogenous sources of MGO and GO

Both enzymatic and non-enzymatic pathways under *in vivo* conditions lead to the formation of MGO and GO.

1.2.1 Enzymetic pathways

The enzymatic pathways represent a series of reactions which are catalyzed by three kinds of enzymes: methylglyoxal synthase, amine oxidase(s), and cytochrome P450 IIE1 isozyme(s). Methylglyoxal synthase catalyzes the transformation of dihydroxyacetone-phosphate (DHA-P) into MGO. The catabolism of proteins through aminoacetone mediated with amine oxidase also produces MGO [21]. Enzymatic oxidations of ketone bodies (acetoacetate and acetone) induce the formation of MGO via the catabolism of acetol by cytochrome P450 IIE1 isozyme(s) [22].

1.2.2 Non-enzymetic pathways

The non-enzymatic pathways during the formation of MGO include decomposition of DHA-P, the Maillard reaction, oxidation of acetol, and lipid peroxidation [23].

Another important production pathway for MGO occurs from the triosephosphate intermediates through glycolytic pathway (**Figure 2**), which includes DHA-P and glyceraldehydes 3-phosphate (GA3P). MGO is formed through two processes: Firstly, a spontaneous non-enzymatic elimination of the phosphate group. Then, decomposition of an ene-diol triose phosphate intermediate that ‘leak’ from the active site of triose phosphate isomerase [24, 25]. The following scheme represents these pathways.

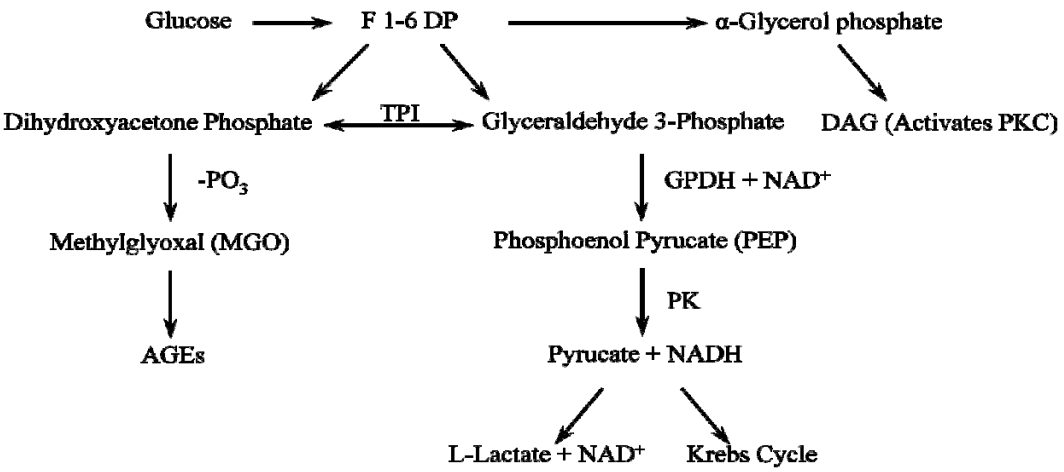

Figure 2. Pathways for producing MGO [24].

Compare to the origin of MGO, the pathways relate to the formation of GO are still poorly understood. Most of our understanding of GO is formed from oxidative fragmentation of Schiff's base, glucose auto-oxidation and degradation, lipid peroxidation, and fructose-phosphate fragmentation (**Figure 3**) [26].

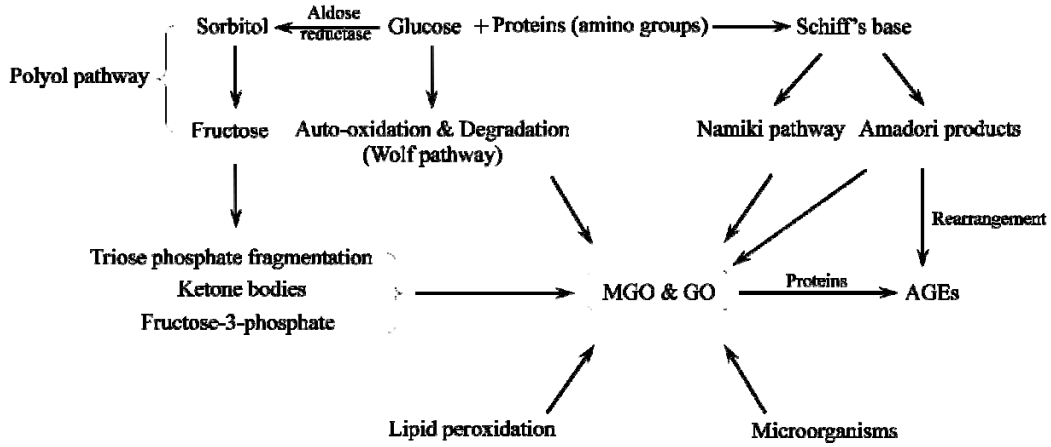

Figure 3. Sources of reactive dicarbonyl compounds (MGO and GO) [26].

2. Role of reactive dicarbonyl compounds in diabetic complications

Advanced glycation irreversibly and progressively modifies proteins and generates the advanced glycation end-products (AGEs). AGEs are considered as one of pathogenic reasons to

develop diabetic complications. The accumulation of reactive dicarbonyl compounds (e.g. MGO and GO) *in vivo* is termed as "carbonyl stress" which plays a significant role in the generation of AGEs **(Figure 4)** [27].

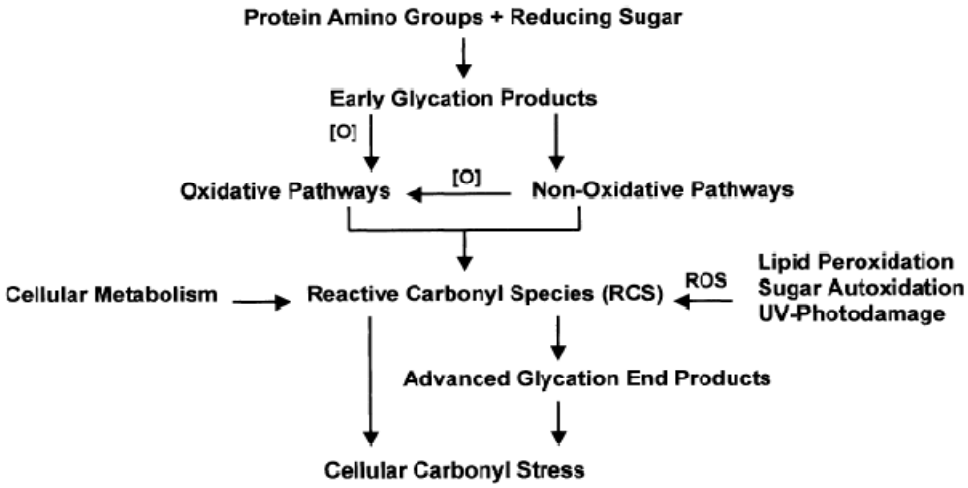

Figure 4. Cellular carbonyl represents stress as a result of glycation, lipid peroxidation, sugar autoxidation, and metabolism. Oxygen-dependent and -independent pathways lead to the formation of various reactive carbonyl species, including α-dicarbonyls, as a key that intermediates for the accumulation of protein damage [27].

2.1 Carbonyl stress and AGEs formation

MGO, GO, and other reactive carbonyl species formed from both glycoxidation and lipoxidation sources as well as the subsequent carbonyl modification of proteins defined as "carbonyl stress" [28], which is a highlighted phenomenon speeded up in diabetic complications. Recently, the carbonyl stress hypothesis underlines the functions of reactive dicarbonyl compounds to modify pathogenic protein, lipid, and DNA and form toxin adducts AGEs. A present study has demonstrated that direct administration of MGO to Sprague Dawley (SD) rats significantly increased the levels of renal Carboxyethyllysine (CEL), systolic blood pressure (SBP), urinary albumin excretion, urinary thiobarbituric acid-reactive substances excretion and the renal nitrotyrosine expression in the kidney compared to non-MG-treated rats. These results

suggested that high level of MGO under in vivo conditions may induce insulin resistance and salt-sensitive hypertension [29].

The formation of AGEs is a complex process in which reducing sugar (e.g., glucose) and proteins are employed as the precursors. The initial reaction between a carbonyl group of the reducing sugar and a free amino group of proteins lead to the formation of fructosamines via a Schiff's base through classic Amadori rearrangement [26]. Then, several reactive dicarbonyl compounds, such as MGO and GO, are formed from Schiff's base and Amadori products by a series of modifications and reactions. New formed reactive dicarbonyl compounds further modify proteins to generate AGEs of various chemical structures by combining amine groups of proteins [30, 31].

Once AGEs were existed under *in vivo* conditions, they can only be degraded follow the degradation of precursor proteins. The most extensive accumulation of AGEs occurs in tissues that contain long-lived proteins, such as crystalline in the lens and collagen in the extracelluar matrix of connective tissues [32]. AGEs can either interfere with physical and chemical properties of proteins or cellular processes. For instance, the accumulation of AGEs decreases the collagen turnover, thereby, renders particular cartilage tissues more prone to mechanical damage [33]. The accumulation of AGEs is promoted in patients with diabetes. Formation of AGEs increases at a greater rate than the increase in blood glucose; this suggests that even moderate elevations in diabetic blood glucose levels result in substantial increases in AGEs accumulation [34, 35].

2.2 Major AGEs identified *in vivo*

MGO and GO are two major dicarbonyl compounds found in our bodies. Especially in patients with both insulin-dependent and non-insulin dependent diabetes, the level of MGO was 2-6 folds higher than those of healthy people [36]. The MGO and GO are extremely reactive and

easily modify lysine, arginine, and cysteine residues on proteins [37]. Several dicarbonyl-derived glycation products *in vivo* have been identified using both chemical and biological assays so far.

2.2.1 AGEs generated from MGO

AGEs derivers from MGO *in vivo* have been identified. The most common measured AGE under *in vivo* conditions was methylglyoxal-lysine dimmer (MOLD), which is formed from the reaction of methylgloxal derivative with two lysine residues [38]. Moreover, Aminoimidazoline imine cross-link was thought to be derived from reaction of arginine and an α-oxoaldimin Schiff base of a lysine residue and MGO [39]. The reaction of MGO with the guanidine group of arginine can also lead to formation of AGEs so known as imidazolone [40]. CEL derived from MGO is found in proteins and in free form *in vivo*[41].

2.2.2 AGEs formed from GO

Under physiological conditions, reactions between GO and protein residues also lead to the formation of AGEs, such as carboxymethyllysine (CML), glyoxal-lysine dimer (GOLD), imidazolone, or Aminoimidazoline imine cross-link. The chemical structures of AGEs derived from both MGO and GO are shown in **Figure 5**.

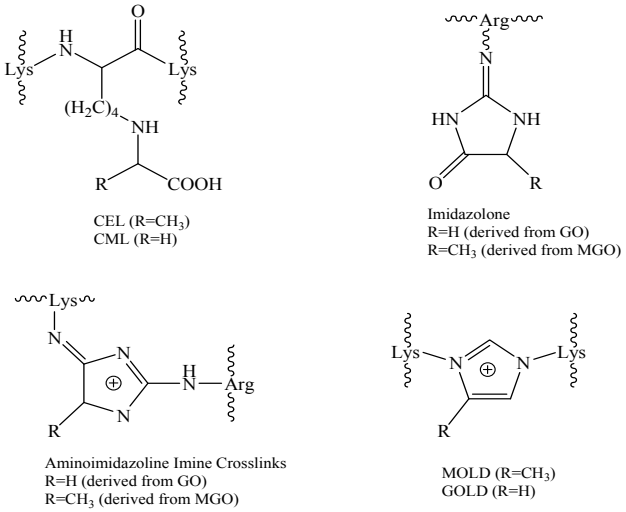

Figure 5. Chemical structures of AGEs derived from MGO and GO.

3. Decreasing the levels of reactive dicarbonyl compounds as an effective approach to prevent the formation of AGEs

The accumulation of AGEs in tissues and organs has been widely discussed as an important factor of developing diabetic complications, such as retinopathy, nephropathy, neuropathy, and macrovascular disease atherosclerosis [8, 34, 35, 42, 43]. To lower the level of AGEs in physiological condition by suppressing the reactive dicarbonyl compounds would be an effective approach to prevent the formation of AGEs.

Aminoguanidine (Pimagedine) is the most well-known AGE inhibitor developed in 1986 [44]. Aminoguanidine quenches toxic reactive dicarbonyl compounds by form the corresponding adducts, 3-amino-1,2,4-triazines, relatively non-toxin adducts [45]. In animal study, the prevention of AGEs formation by aminoguanidine delays evolving the microvascular lesions in diabetic animals [46]. Although Aminoguanidine performed very well on suppressing AGE formation, the drug is not being further advanced due to the side effects in phase III clinical trials in patients with diabetes [47].

Metformin as an oral antihyperglycemic agent is usually used for the treatment of non-insulin-dependent diabetes mellitus (NIDDM). The trapping of MGO and GO by metformin was studied by *Daniel and Nicolas in 1999*. Their research strongly suggested that metformin can effectively quench MGO and GO to form subsequent adducts: triazepinoe and non-methylated trazepinoe under in vitro condition. More recently, *Beisswenger and Ruggiero-Lopez* further proved the scavenging effect of metformin by decreasing the MGO level *in vivo* [48].

In addition, several other potential drug candidates have been tested on AGEs inhibition by sequestering reactive dicarbonyl compounds, such as pyridoxamine (Pyridorin®) and 4-oxo-N-

phenyl-4,5-dihydro-2-[(1-methylethylidene)hydrazino]-5-thiazoleacetamide (OPB-9195). The chemical structures of these potential candidates are showed in **Figure 6** [44].

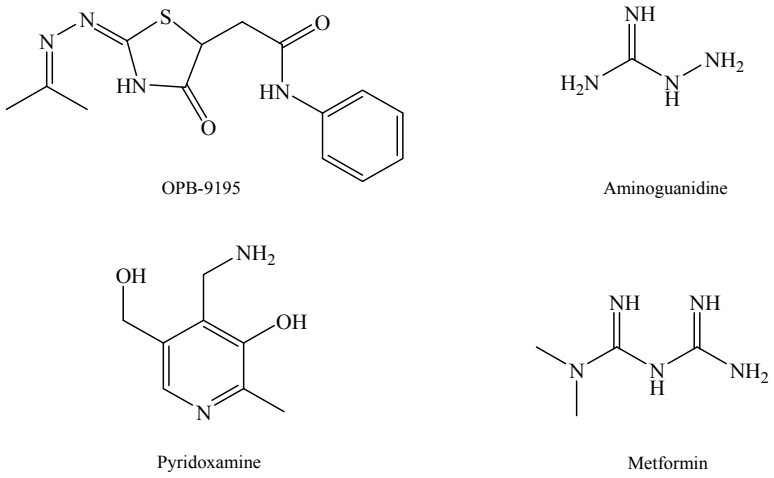

Figure 6. Representative advanced glycation end product (AGE) inhibitors

4. Effects of dietary flavonoids on diabetes

Flavonoids are polyphenolic compounds that are ubiquitous in nature and many of which occur in fruits, vegetables and beverages (tea, coffee, beer, wine and fruit drinks). The flavonoids have aroused considerable interest recently because of their potential beneficial effects on human health. They have been reported to reduce the risk of cancers, cardiovascular disease, asthma, as well as diabetes. According to chemical structure, flavonoids can be categorized into flavonols, flavones, flavanones, isoflavones, catechins, anthocyanidins and chalcones. Flavonoids from all six categories have been shown to have antidiabetic effect in animals or *in vitro* studies. The well-known anti-oxidant activity of flavonoids have the potential to suppresses the oxidative stress and facilitate the detoxification of dicarbonyl species (**Figure 7)** [49].

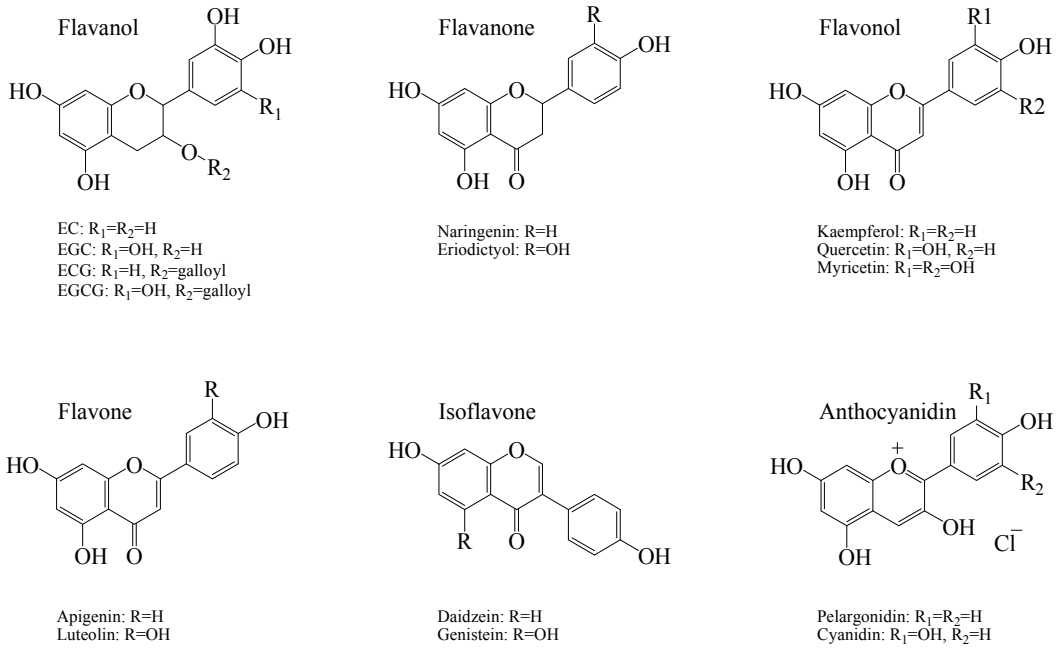

Figure 7. Chemical structures of major dietary flavonoids [49].

4.1 Human study

The effects of dietary flavonoids on diabetes have received increasing attention as human studies' data accumulated.

A prospective study in Finland showed that the intake of some specific types of flavonoids including quercetin and myricetin was inversely associated with risk of incident of type 2 diabetes in Finnish men and women (age > 40 y) [50]. Moveover, a recent study suggested that green tea promotes glucose metabolism in healthy humans in oral glucose tolerance tests [51]. Antihyperglycemic effect of oolong tea has been tested in human study: compared with water control group, plasma glucose and fructosamine levels of type 2 diabetes patients decreased significantly after daily consumption of oolong tea [52].

4.2 Animal study

Several animal studies have shown that dietary flavonoids had potential anti-diabetes effect. For instance, the significant reductions of serum glucose were observed in EGCG-treated Sprague-Dwley rats, male lean and obese Zucker rats [41]. Moreover, daily treatment of green tea to rats with streptozotocin (STZ)-induced diabetes showed inhibition of diabetic cataracts by lowering plasma and lens glucose levels. The same phenomenon was noted in a black tea treatment group [53]. Green tea lowered blood glucose concentrations in the genetically diabetic db/db mice 2-6 h after administration at 300 mg/kg bw; whereas, no effect was observed in control mice [51]. The reduction of carbohydrate absorption from the intestine of rats with a saccharide-supplemented by EGCG or green tea is based upon suppression of the activity of intestinal α-amylase, sucrase, or α-glucosidase [53].

Besides flavonoids from tea, naringenin and its glycosides, quercetin, luteolin glycoside, genistein, and diacylated anthocyanins have also been performed significant effecs on reducing blood glucose levels in streptozotocin (STZ) - induced diabetic rats [54-57]. Moreover, several studies have shown phloretin and phloridzin inhibit the intestine glucose absorption in a high-starch diet induced rat.

5. Effects of dietary flavonoids on diabetes-related complications and AGEs formation

The ability of preventing diabetic-related complications by dietary flavonoids has been tested in several studies. For instance, oral administration of tea catechins retarded the progression of functional and morphological changes in the kidney of STZ-induced diabetic rats [58]. Also, the effects of ameliorating glucose toxicity, renal injury, and thus alleviating renal damage by (-)-epigallocatechin gallate (EGCG) have been pointed out in diabetic nephropathy model rats [59].

The detailed mechanisms for the prevention of diabetic complications by flavonoids are remaining for further studies. Several studies showed that those effects could partially because of

the inhibition of AGEs formation. *Wu et al*. reported the inhibitory effect of naturally occurring flavonoids on the formation of AGEs. Kaempferol, luteolin, naringenin, qucertin, rutin, and tea catechins were screened in their study, in which, (-)-epicatechin gallate (ECG), EGCG, luteolin, and rutin showed significant effects to inhibit the formation of AGEs under *in vitro* condition. *Rutter* et. al. also reported that green tea extract was able to delay collagen aging in C57Bl/6 mice by blocking AGEs formation and collagen cross-linking [60]. In addition, EGCG showed effects of reducing renal AGEs accumulation and its related protein expression in the kidney cortex based upon STZ-induced diabetic nephropathy model rats [50]. *In vitro* study, *Lai* et al. demonstrated green tea polyphenols dose-dependently inhibited AGE-stimulated proliferation and p44/42 mitogen-activated protein kinase (MAPK) expression of rat vascular smooth muscle cells (VSMCs) [61]. *Yen et al* have tested vanillic acid on suppressed methylglyoxal-induced Neuro-2A cell apoptosis via inhibition of glycation mechanisms including ROS, p38 and JNK, PKC and p47phox, and methylglyoxal-derived CML formation.

6. Methodologies for quantification of reactive dicarbonyl compounds

6.1 Sample preparation

Since the insolubility of proteins during chromatographic analysis and the necessity of the reversibly bound MGO liberation from proteins, protein precipitation plays a significant role in MGO quantification process. Perchloric acid (PCA) is widely used in the protein precipitation procedure because of the low pH that would prevent degradation of dihydroxyacetone phosphate and 3-phosphate to MGO through phosphate elimination [2]. However, PCA can increase MGO level due to oxidative degradation of nucleic acids to MGO in biological samples, thereby causes inaccurate quantification [62]. Since Triflouroacetic acid (TFA) could easily be removed by evaporation or freeze drying, which is often used for deproteinization of human plasma samples.

In addition, deproteinization with methanol is not recommended because of the large solvent volumes and extended periods of time requirements [63].

6.2 Analytical methods

6.2.1 High Performance Liquid Chromatography (HPLC)

Since MGO cannot be directly measured, most HPLC methods are based on MGO derivatization into quinoxaline adducts with diamino derivatives of benzene or naphthalene. These quinoxaline can easily be monitored either by UV detector at 300-360 nm or by fluorescent detector with excitation wavelengths at 300-360 nm and emission wavelength at 380-450 nm [64].

HPLC method where MGO was derivatized into the corresponding fluorescent pteridine derivative with 6-hydroxy-2, 4, 5-triaminopyrimidine (TRI) or 2-ace-trlthiazolidine by cysteamine have also been described. The main disadvantage is that the new derivatization can form two kinds of isomers for MGO and affect the accurate of quantification [65].

More recently, electrospary ionization liquid chromatography/mass spectrometry (ESI/LC/MS) method has been developed based upon the quantification of dicarbonyl adducts with 2, 3-diaminonaphthalene. This method offers the advantage of greater specificity for measuring dicarbonyl compounds [66]. However, this method requires time-consuming liquid-liquid or solid-phase extraction (SPE) and considerable quantities of highly pure, usually toxic, organic solvents.

Generally, injection of the sample to the instrumentation would be the last step of MGO quantification. However, the concentration of MGO in samples might be too low to measure. So the pre-concentration of the sample is often necessary. Usually, the liquid-liquid extraction and

SPE will be used and later followed by evaporation of organic solvent or freeze-drying. HPLC analysis was usually performed on the reverse phase C18 columns and eluted with water solutions of acids or buffers in combination with methanol or acetonitrile under gradient or isocratic conditions.

6.2.2 Gas Chromatography (GC)

GC methods were relied on MGO derivatiztion by 1,2-diaminobenzene with detection either on mass spectrometry/selected ion monitor (MS/SIM) or on specific nitrogen phosphorus detector (NPD), and by o-(2,3,4,5,6-pentafluorobenzyl) hydroxylamine hydrochloride (PFBOA) detection either on MS/SIM detector, electron-capture detector (EDC), NPD, or flame photometric detector [67]. The development of GC method offers the advantage of applying less sample treatment and low-price equipment to perform highly specific measurements. The time-consuming extraction process and toxic, organic solvents application is considered to be the disadvantages of GC method. The GC analysis is usually performed on fused-silica capillary columns with helium as carrier gas.

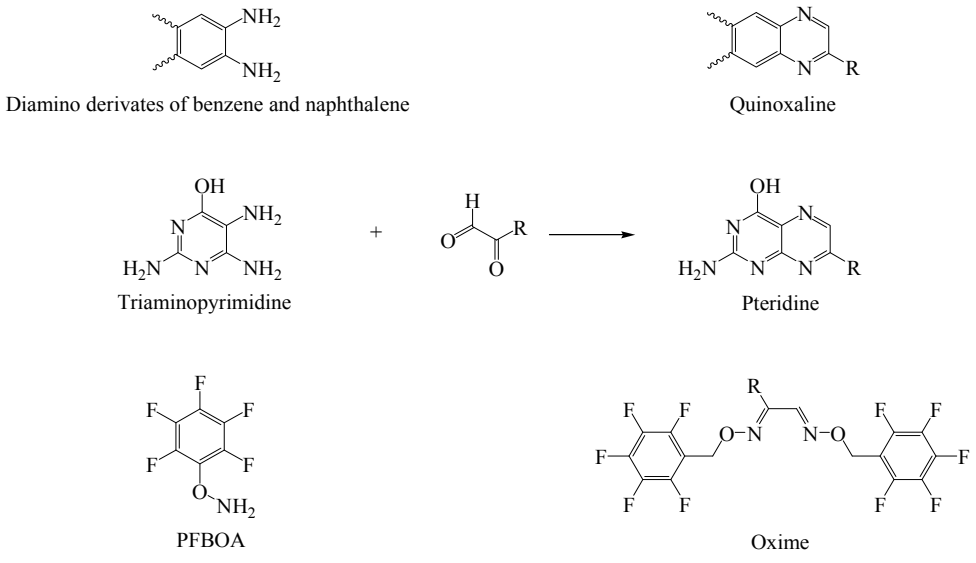

Figure 8. Derivatization of MGO, GO with diamino derivates of benzeneand naphthalene, triaminopyrimidine, and PFBOA [65].

7. Methodologies for quantification of AGEs

Although there are experimental evidences for AGEs accumulation with age and under certain pathological states such as diabetes, it is difficult to compare results between laboratories. Moreover, there is now a number of AGEs, which are structurally heterogeneous making it difficult to ensure that the AGEs detected is relevant to the complications observed *in vitro* or *in vivo*. To date AGEs measurement is confined to investigative laboratories. Currently there is no commonly accepted or widely used method to detect AGEs, nor any commercially available kits. Although there is no universally established unit of measurement, it has recently been proposed to adopt a universal unit of measurement for different laboratories to compare results. The lack of internal standards leaves assays open to error which require a high degree of accuracy and reproducibility for each sample run. Currently the most common methods used for detection are HPLC [68], LC/MS [69], enzyme linked immunosorbent assay (ELISA) [70, 71] and immunohistochemistry [72]. Recently, a monoclonal antibody which recognizes CML, called 6D12, has become commercially available [73].

7.1 Fluorescence

The fluorescent property of AGEs was found by *Monnier* [74], who demonstrated that fluorescent pigments show similar fluorescence spectra to AGEs. Since then, the measurement of fluorescence intensity after excitation at 370 nm, at emission 440 nm was widely used for characterizing and quantifying purpose. Fluorescence was expressed as the relative fluorescence intensity in arbitrary units (A.U.) [75]. However, measurement of AGEs by means of fluorometric analysis is limited due to its low specificity.

7.2 HPLC methods

Due to the structurally heterogeneous properties of AGEs, HPLC methods are usually used for quantify and identify the amino acid residues from enzymatic digestion of the most severely glycated portion of proteins or conjugated amino acids with reactive dicarbonyl intermediates under *in vitro* condition. Different of sample preparation, separation, and detection methods should be considered based on the structural properties of each specific AGEs during HPLC method development.

For instance, determination of CEL in glucose-modified bovine serum albumin (AGE-BSA) by HPLC may be affected by co-elution with CML due to the similar chemical structure of those two AGEs. A HPLC method coupled with a styrene-divinylbenzene co-polymer resin coupled with sulfonic group cation exchange column followed by a ninhydrin post-column derivatization and detection by fluorescence (ex. 271nm/em. 503nm) was developed for the quantification of CEL-contents of modified BSA by *Pyoji N* and *Seikoh H* et al. [75].

7.3 LC-MS/MS methods

Liquid chromatography-tandem mass spectrometry (LC-MS/MS) is currently the method of choice for the analysis of AGEs. For instance, a stable-isotope-dilution LC-MS/MS method have been widely used to analyze CML and CEL, two major nonenzymetic chemical modifications on tissue proteins, that serve as biomarkers of oxidative stress resulting from sugar and lipid oxidation [76].

Since high AGE concentrations reflect the production of AGE-modified proteins which, being chemically altered, show different biological activity, activating a macrophage response with consequent internalization and digestion [77]. AGE-modified proteins can then generate a series of AGE-modified and highly reactive peptides, which react with plasma lipoprotein (low density lipoprotein, LDL) to form AGE-modified LDL and cross-links with collagen. In order to

obtain information on the preferential glycation sites of the protein, LC-MS/MS methods were also used to perform the structural elucidation [74].

7.4 ELISA

To investigate the histological localization and obtain more specific level of AGEs *in vivo*, few immunochemical quantification methods for specific AGEs have been developed. CML and CEL are two widely studied AGEs by using immunochemistry method. The monocolonal anti-AGE antibody 6D12 prepared in mice has demonstrated the presence of AGEs-modified proteins in several human tissues, such as human lens, renal proximal tubules in patients with diabetic nephropathy and chronic renal failure, peripheral nerves of diabetic neuropathy, and atherosclerotic lesions of arterial walls. However, some of the CML detected by monoclonal anti-CML antibody **(**6D12) and conventional polyclonal anti-CML antibody (CPC) might cross-react with CEL due to the structural similarity.

PREVIOUS STUDY

In previous study, we found that EGCG could rapidly trap both MGO and GO under neutral or alkaline conditions. Our data showed that EGCG was more reactive than lysine and arginine in terms of trapping MGO or GO, indicating that EGCG has the potential to compete with lysine and arginine *in vivo* and therefore prevent the formation of AGEs. In addition, we also found that EGCG was more reactive at trapping MGO than the pharmaceutical agent, aminoguanidine, which has been shown to inhibit the formation of AGEs by trapping of reactive dicarbonyl compounds *in vivo*. (**Figure 9**)

We have purified two major products, EGCGMGO-1 and -2, from the reaction between EGCG and MGO at a 3:1 mole ratio. Their structures were identified as the mono-MGO adducts

of EGCG with the MGO conjugated at position 8 of the EGCG A-ring for both compounds. Our results clearly indicate that the major active site of EGCG is at position 6 and 8 of the A-ring and that the gallate ring does not play an important role in the trapping of reactive dicarbonyl species.

Based on our observation, a mechanism of EGCG trapping MGO to form mono- and di-MGO adducts is proposed (**Figure 10**) [78]. The slightly alkaline pH can increase the nucleophilicity at position 6 and 8 of the A-ring of EGCG, facilitating the addition of MGO at these two positions to form mono- and di-MGO adducts.

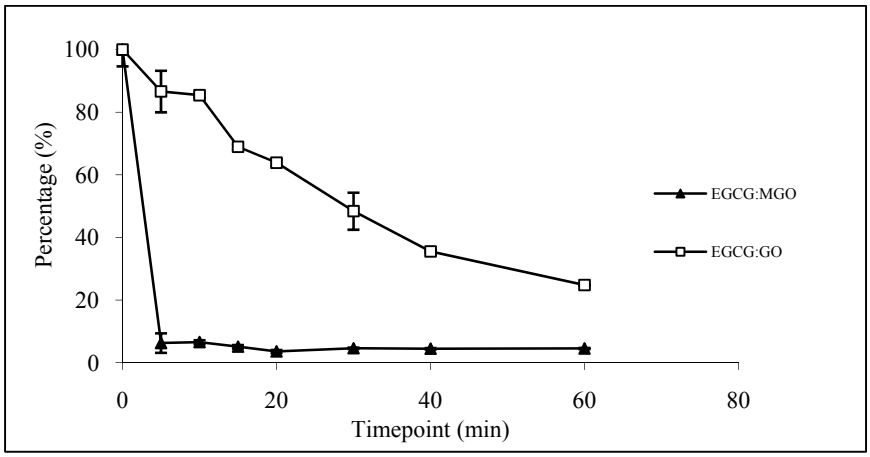

Figure 9. Trapping of MGO and GO by EGCG under physiological conditions (37 °C, pH 7.4).

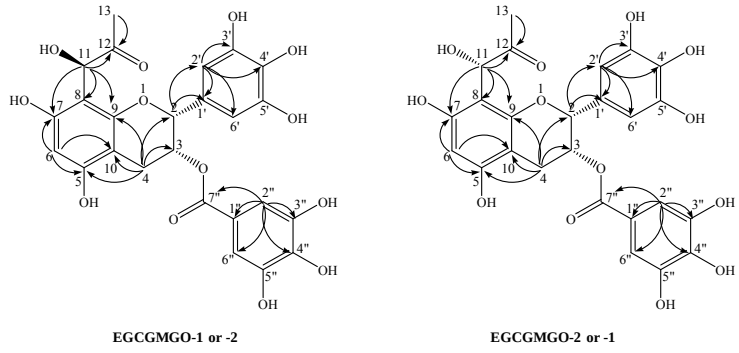

Figure 10. Significant HMBC (H-C) correlations of EGCGMGO-1 and EGCGMGO-2.

HYPOTHESIS AND RESEARCH OBJECTIVES

Many studies have shown that dietary flavonoids, which are widely distributed in fruits, vegetables, grains, and beverages, such as tea, coffee, and wine, are strong antioxidants and may prevent diabetes and its complications. However, the mechanisms by which dietary flavonoids prevent the development of diabetic complications are unclear. It has been observed *in vitro* that dietary flavonoids may inhibit the formation of AGEs by trapping reactive dicarbonyl compounds. A recent study found that flavonoids containing vicinyl dihydroxyl groups, such as quercetin and myricetin, could significantly decrease the level of GO during the auto-oxidation of glucose *in vitro*. These authors also found that rutin and its metabolite, quercetin, could effectively inhibit GO-derived AGEs formation during glycation of collagen I by glucose. Since luteolin, rutin, and quercetin have the same A-ring structure as that of EGCG, they may have the same mechanism to trap reactive dicarbonyl species and form A-ring MGO or GO adducts. However, the reaction between dietary flavonoids and reactive dicarbonyl compounds needs to be further characterized. It is also important to know whether dietary flavonoids can effectively inhibit the formation of AGEs by trapping reactive dicarbonyl compounds *in vivo*. Thus, our hypothesis is that **dietary flavonoids, such as phloretin and phloridzin from apple, can scavenge reactive dicarbonyl compounds (e.g. MGO and GO) and thus prevent the formation of AGEs and the development of diabetic complications**. In my research, this hypothesis will be tested by **(1) studying the scavenging effect of MGO and GO by apple polyphenols: phloretin and phloridzin and identifying the major carbonyl adducts in buffer solutions; and (2) Studying the structure-activity relationship of dietary flavonoids to trap dicarbonyl species and their possible implication for inhibition of the formation of advanced glycation-end products.**

MATERIALS AND METHODS

1. Study the trapping effects of MGO and GO by apple polyphenols: phloretin and phloridzin.

1.1 Materials.

Phloretin, phloridzin, methylglyoxal (40% in water), glyoxal (40% in water), quinoxaline, 2-methylquinoxaline, 1,2-diaminobenzene, CD_3OD, RP C-18 silica gel, Sephadex LH-20 gel, and TLC plates (250 μm thickness, 2-25 μm particle size) were purchased from Sigma (St. Louis, MO). HPLC-grade solvents and other reagents were obtained from VWR Scientific (South Plainfield, NJ). HPLC-grade water was prepared using a Millipore Milli-Q purification system (Bedford, MA).

1.2 Kinetic study of the trapping of MGO or GO by phloretin or phloridzin under physiological conditions.

MGO (0.33 mM) or GO (0.33 mM) was incubated with 1 mM phloretin or phloridzin in a pH 7.4 phosphate buffer solution (100 mM) at 37°C and shaken at 40 rpm speed for 0, 10, 30, 60, 120, 240, 480, 1440min. Then, to each triplicated vial at each time point, 1μL acetic acid was added to stop the reaction and 100 mM DB was added next to derivatize the remaining MGO or GO using our previous method [78].

1.3 HPLC analysis.

The levels of methylquinoxaline and quinoxaline were analyzed using our previous HPLC method with slight modification [78]. In brief, the HPLC system consisted of a Waters 717 refrigerated autosampler, a HITACHI L-6200 Inteligent pump, and a Waters 490E programmable multiwavelength UV-Vis detector. A Supelcosil C18 reversed-phase column (150 mm x 4.6 mm

inner diameter; Supelco Co., Bellefonte, PA) was used with a flow rate of 1 mL/min. The binary mobile phase system was consisted by 5% aqueous acetonitrile with 0.2% acetic acid as A and 95% aqueous acetonitrile with 0.2% acetic acid as B. The column eluted with a binary gradient system: 100% ~ 65% A from 0 min to 5 min; 65% ~ 60% A from 5 min to 15 min; 60% ~ 0% A from 15 min to 20 min; then 100% A from 21 min to 30 min. The injection volume was 50 μL for each sample solution. The wavelength of UV detector was set at 280 nm for methylquinoxaline and 313 nm for quinoxaline with 100 ng/mL as the limit of detection and 1 μg/mL as the limit of uantification for both methylquinoxaline and quinoxaline.

1.4 LC/MS analysis.

A Finnigan LC/ESI-MS System equipped with a Surveyou MS pump, a Surveyou refrigerated autosampler, and a LTQ linear ion trap mass detector (ThermoFinigan, San Jose, CA) incorporated with electrospray ionization (ESI) interface. A Gemini C18 column (50 × 2.0 mm i.d., 3 μm, Phenomenex) was used for the analysis of the reaction products with a flow rate of 0.2 mL/min. The binary mobile phase system consisted of 5% aqueous methanol with 0.2% acetic acid as A and 95% aqueous methanol with 0.2% acetic acid as B. The column eluted with isocratic phase A for 5 min followed by the gradient progress: 100% ~ 70% A from 5 min to 20 min; 70% ~ 0%A from 20 min to 40 min; then 100% A from 41 min for 10 min. The injection volume was 10 μL for each sample solution. The column temperature was maintained at 20ºC. The LC elute was introduced into the ESI interface. The negative ion polarity mode was set for ESI ion source with the voltage on the ESI interface maintained at approximately 5 kV. Nitrogen gas was used as the sheath gas at a flow rate of 30 arb units and the auxiliary gas at 5 arb units, respectively. The structural information of phloretin, phloridzin, and the major MGO or GO adducts was obtained by tandem mass spectrometry (MS/MS) through collision-induced dissociation (CID) with a relative collision energy setting of 35%.

1.5 Studying the formation of MGO or GO adducts of phloretin or phloridzin using LC/MS.

Phloretin or phloridzin (1.0 mM) was incubated with different concentrations of MGO or GO (0.33, 1.0, 3.0, and 100.0 mM) in a pH 7.4 phosphate buffer solution at 37 °C for 60 min, respectively. Then, 10 μL samples were taken and transferred to vials already containing 190 μL of a solution containing 0.2% ascorbic acid and 0.05% EDTA, to stabilize ploretin or phloridzin and related MGO or GO adducts. These samples were immediately analyzed or stored at -80 °C before analyzing with LC/MS.

1.6 NMR analysis.

^{1}H (400 MHz), ^{13}C (100 MHz), and all 2D NMR spectra were acquired on a Varian 400 instrument (Varian Inc., Palo Alto, CA) at 25 °C. The DEPT-135 ^{13}C NMR spectra were obtained on a Bruker DRX 500 NMR instrument at 25 °C using a Nalorac 3-mm ^{1}H-^{13}C dual probe. Compounds were analyzed in CD_3OD in a 3-mm I.D. tube. ^{1}H-^{13}C HMQC (heteronuclear multiple quantum correlation) and HMBC (heteronuclear multiple band correlation) experiments were performed as described previously [79]. The ^{1}H and ^{13}C chemical shift assignments were referenced internally to TMS at 0 ppm.

1.7 Purification of the major mono-MGO adduct of phloridzin.

Phloridzin (0.5 g, 1.06 mmol) and MGO (4.132g, 57.34 mmol) were dissolved in a 300 mL phosphate buffer (100 mmol/L, pH 7.4) and then kept at 37 °C for 60 min. After extraction with ethyl acetate and the evaporation of the solvent *in vacuum*, the residue was loaded into a Sephadex LH-20 column eluted with ethanol to obtain mono-MGO conjugated phloridzin (130 mg). ^{1}H and ^{13}C NMR data of phloridzin and mono-MGO conjugated phloridzin were listed in **Table 1**.

2. Study the structural-activity relationship for trapping dicarbonyl species by dietary flavonoids

2.1 Materials.

Quercetin, luteolin, epicatechin, genistein, daidzein, naringenin, apigenin, gallic acid, phloroglucinol, methylglyoxal (40% in water), quinoxaline, 2-methylquinoxaline, 1,2-diaminobenzene, and human serum albumin (HSA) were purchased from Sigma (St. Louis, MO). Pyrogallol, pyrocatechol, and resorcinol were purchased from Fisher (Pittsburgh, PA). HPLC-grade solvents and other reagents were obtained from VWR Scientific (South Plainfield, NJ). HPLC-grade water was prepared using a Millipore Milli-Q purification system (Bedford, MA).

2.2 Kinetic study of the trapping of MGO by dietary flavonoids under physiological conditions.

MGO (0.33 mM) was incubated with 1 mM quercetin, luteolin, epicatechin, genistein, daidzein, naringenin, apigenin, gallic acid, phloroglucinol, pyrogallol, pyrocatechol, and resorcinol in a pH 7.4 phosphate buffer solution (100 mM) at 37°C and shaken at 40 rpm speed for 0, 10, 30, 60, 120, 240, 480, 1440min. Afterward, 200 μL of reacted mixtures were collected at each time point, 1μL of acetic acid was added to stop the reaction and 100 mM DB was used for the derivatization of the remaining MGO using our previous method [78].

2.3 HPLC analysis.

The levels of methylquinoxaline was analyzed using our previous HPLC method with slight modification [78]. In brief, the HPLC system consisted of a Waters 717 refrigerated autosampler, a HITACHI L-6200 Inteligent pump, and a Waters 490E programmable multiwavelength UV-Vis detector. A Supelcosil C18 reversed-phase column (150 mm x 4.6 mm inner diameter; Supelco Co., Bellefonte, PA) was used with a flow rate of 1 mL/min. The binary mobile phase system was

consisted by 5% aqueous acetonitrile with 0.2% acetic acid as A and 95% aqueous acetonitrile with 0.2% acetic acid as B. The column eluted with a binary gradient system: 100% ~ 65% A from 0 min to 5 min; 65% ~ 60% A from 5 min to 15 min; 60% ~ 0% A from 15 min to 20 min; then 100% A from 21 min to 30 min. The injection volume was 50 μL for each sample solution. The wavelength of UV detector was set at 280 nm for methylquinoxaline and 313 nm for quinoxaline with ~100 ng/mL as the limit of detection and 1 μg/mL as the limit of quantification for both methylquinoxaline.

3. Study the inhibitory effects on the formation of AGEs by dietary flavonoids

3.1 Materials

Phloretin, phloridzin, genistein, methylglyoxal (40% in water), quinoxaline, 2-methylquinoxaline, 1, 2-diaminobenzene, human serum albumin were purchased from Sigma (St. Louis, MO). LC/MS-grade solvents and other reagents were obtained from Fisher Scientific (Pittsburgh, PA). HPLC-grade water was prepared using a Millipore Milli-Q purification system (Bedford, MA).

3.2 Effects of MGO on the formation of AGEs with human serum albumin

HSA (1.4 mg/ml) was incubated with MGO solutions (100 μM, 250 μM, 500 μM, and 1.0 mM) in 0.2 M PBS buffer (pH 7.4) at 37°C. 0.3ml of Streptomycin and penicillin mixed solution was added before incubation to prevent the growth of bacterials. 400 μl of reaction mixture was collected and frozen at different timepoints (0, 1, 2, 4, 7, 14, 21 days). Fluorescence was read at an excitation/emission wavelength of 370/440 nm, which is characteristic of AGEs.

3.3 Kinetic study of the inhibitory effects on the formation of AGEs by genistein

HSA (1.4mg/ml) was incubated with MGO (500 μM) in the presence of genistein (1.5 mM) in PBS buffer, pH 7.4 at 37°C, respectively. Genistein (1.5 mM) was also incubated with MGO

(500 μM) in the presence of HSA (0 and 1.4 mg/mL) for the background screen. 0.3ml of Streptomycin and penicillin mixed solution was added before incubation to prevent the growth of bacterials. 400 μl of reaction mixture was collected and frozen at different timepoints (0, 2, 4, 8, 48, 144, 240, and 408 hr). AGEs levels were quantified using fluorescence at an excitation/emission wavelength of 370/440 nm, which is characteristic of AGEs.

3.4 Kinetic study of the inhibitory effects on the formation of AGEs by phloretin and phloridzin

HSA (1.4mg/ml) was incubated with MGO (500 μM) in the presence of PE and PZ (0 μM, 250 μM, 500 μM, 1.0 mM, and 2.0 mM) in PBS buffer, pH 7.4 at 37°C, respectively. 0.3ml of Streptomycin and penicillin mixed solution was added before incubation to prevent the growth of bacterials. 400 μl of reaction mixture was collected and frozen at different timepoints (0, 1, 2, 4, 7, 14, 21 days). AGEs levels were quantified using fluorescence at an excitation/emission wavelength of 370/440 nm, which is characteristic of AGEs.

3.5 LC/MS analysis

LC/MS analysis was carried out with a Thermo-Finnigan Spectra System which consisted of an Accela high speed MS pump, an Accela refrigerated autosampler, an Accela photodiode array (PDA) detector, and an LCQ Fleet ion trap mass detector (Thermo Electron, San Jose, CA, USA) incorporated with electrospray ionization (ESI) interfaces. A 50 × 2.0 mm i.d., 3 μm Gemini C18 column (Phenomenex, Torrance, CA, USA) was used for separation at a flow rate of 0.2 mL/min. The column was eluted with 100% solvent A (5% aqueous methanol with 0.2% acetic acid) for 5 min, followed by linear increases in B (95% aqueous methanol with 0.2%acetic acid) to 50% from 5 to 10 min, to 65% from 10 to 25 min, to 100% from 25 to 40 min, and then with 100% B from 40 to 45 min. The column was then re-equilibrated with 100% A for 5 min. The LC eluent was introduced into the ESI interface. The negative ion polarity mode was set for ESI ion source

with the voltage on the ESI interface maintained at approximately 5 kV. Nitrogen gas was used as the sheath gas at a flow rate of 30 arb units and the auxiliary gas at 5 arb units, respectively. The structural information of phloretin, phloridzin, and the major MGO or GO adducts was obtained by tandem mass spectrometry (MS/ MS) through collision-induced dissociation (CID) with a relative collision energy setting of 35%. Data acquisition was performed with Xcalibur version 2.0 (Thermo Electron, San Jose, CA, USA).

RESULTS AND DISCUSSION

1. Study the trapping effects of MGO and GO by apple polyphenols: phloretin and phloridzin.

1.1 Trapping of MGO or GO by phloretin and phloridzin under physiological conditions.

We found that both phloretin and phloridzin could effectively trap MGO or GO under physiological conditions. More than 80% MGO was trapped within ten minutes and 68% GO was trapped within 24 h by phloretin (**Figure 11**). Phloridzin also had strong trapping efficiency by quenching more than 70% MGO and 60% GO within 24 h (**Figure 12**).

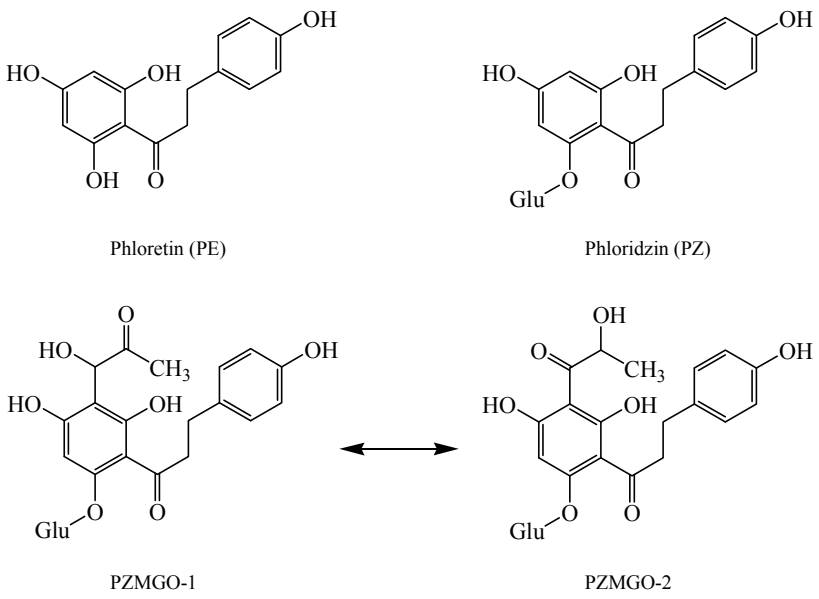

Figure 11. Chemical structures of phloretin (PE), phloridzin (PZ) and its mono-MGO adducts.

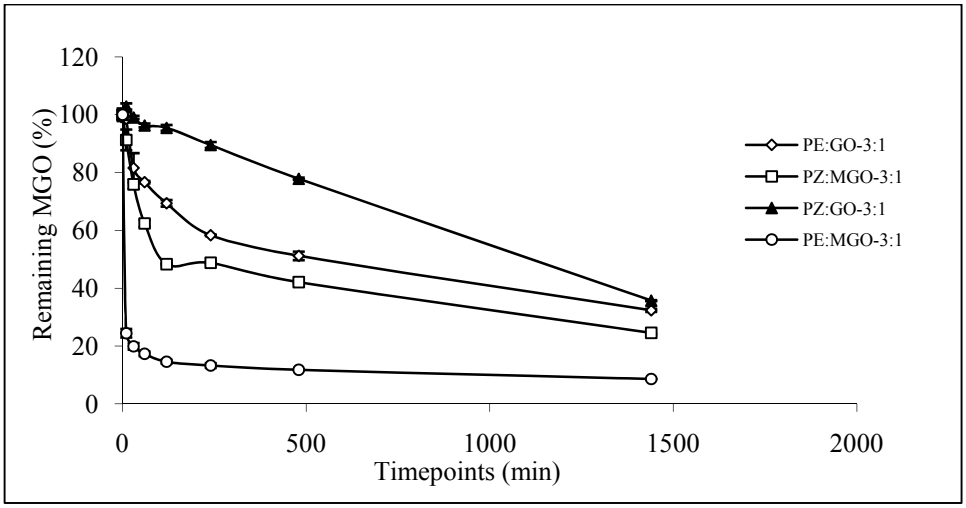

Figure 12. Trapping of MGO and GO by phloretin and phloridzin in phosphate buffer (pH 7.4, 37 °C). MGO (0.33 mM) or GO (0.33 mM) was incubated with 1 mM phloretin and phloridzin in pH 7.4 phosphate buffer solutions at 37 °C for 10, 30, 60, 120, 240, 480 and 1440 min, respectively.

1.2 Studying the formation of MGO and GO adducts of phloretin by LC/MS.

The reaction mixtures of phloretin with MGO or GO under four different ratios (3:1, 1:1, 1:3 and 1:100) were analyzed by LC/MS (**Figures 13 and 14**). The structural information of these products was obtained using LC/MS/MS analysis under selective ion monitoring (SIM) mode (**Figures 15 and 16**).

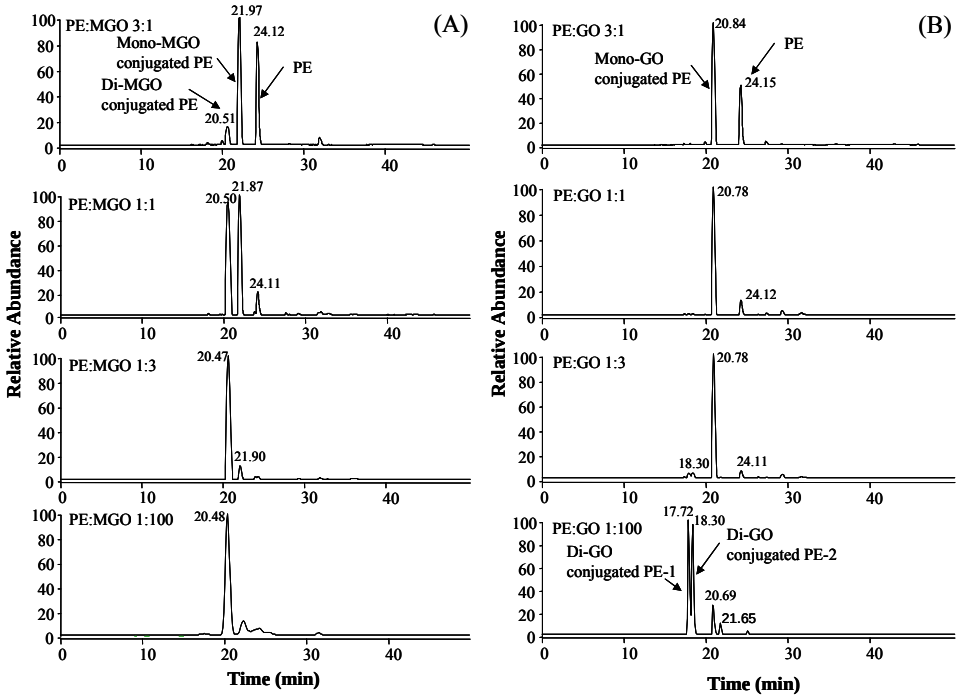

Figure 13. LC chromatograms of phloretin after incubation with different ratios of (A) MGO (3:1, 1:1, 1:3, and 1:100) and (B) GO (3:1, 1:1, 1:3 and 1:100) for 60 min, respective.

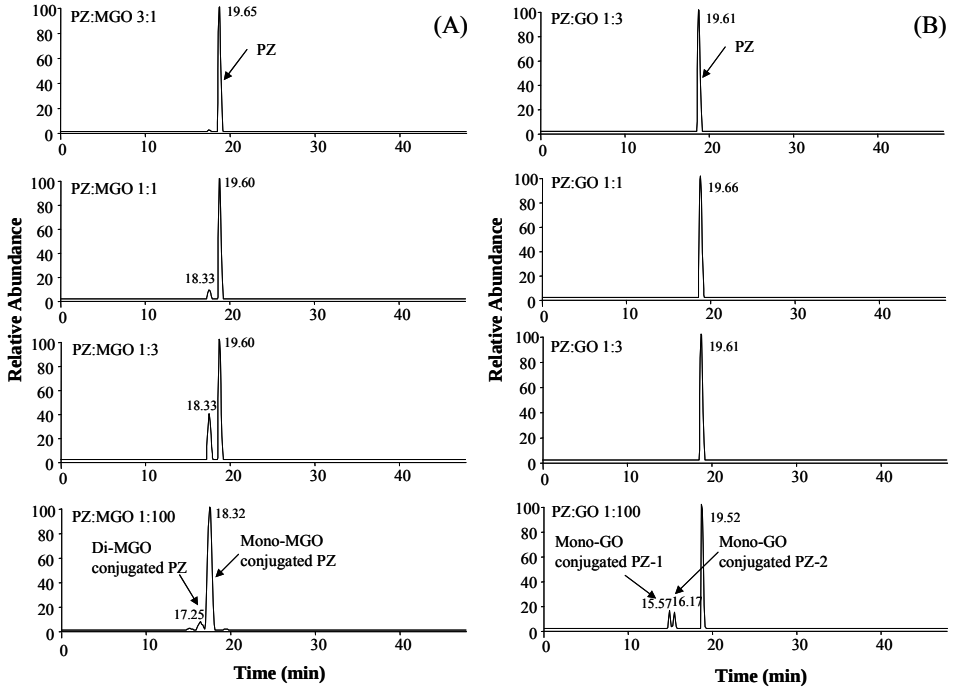

Figure 14. LC chromatograms of phloridzin after incubation with different ratios of (A) MGO (3:1, 1:1, 1:3, and 1:100) (B) GO (3:1, 1:1, 1:3 and 1:100) for 60 min, respectively.

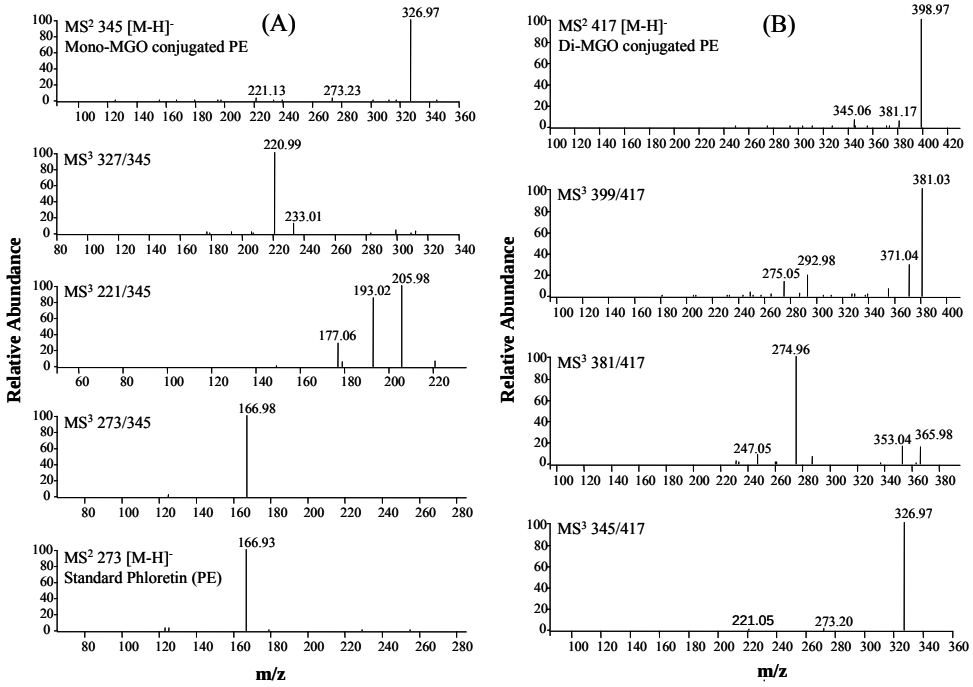

Figure 15. Tandem MS/MS spectra of (**A**) mono-MGO, phloretin standard, and (**B**) di-MGO adducts of phloretin.

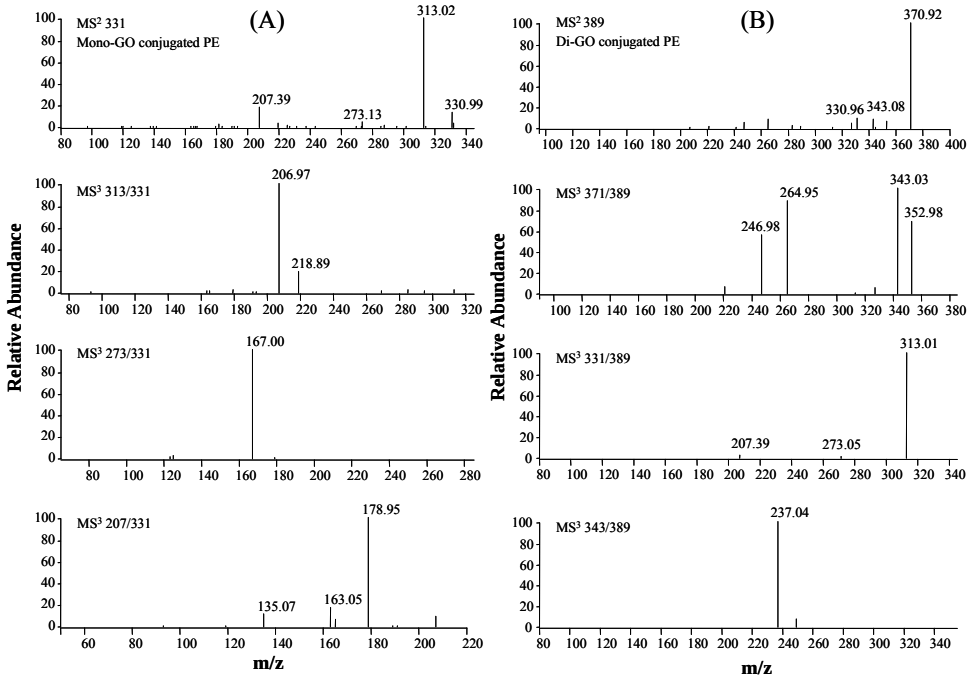

Figure 16. Tandem MS/MS spectra of (**A**) mono-GO and (**B**) di-GO adducts of phloretin.

After 1 h incubation of phloretin with MGO (3:1 ratio), two major new peaks appeared in the LC chromatogram (**Figure 13**). One had the molecular ion m/z 345 ($[M-H]^-$, RT: 21.97 min), and the other had the molecular ion 417 ($[M-H]^-$, RT: 20.51 min) (**Figures 12** and **14A**). The peak at 21.97 min had the fragment ion m/z 273$[M-72-H]^-$, which lost one MGO (m/z 72) molecule, and the MS/MS spectrum of this daughter ion (MS3 273/345) was identical to the MS/MS spectrum of the standard phloretin (MS^2 273) (**Figure 15A**). All of these features indicated that this product was the mono-MGO conjugate of phloretin. The MS/MS spectrum of the most abundant daughter ion m/z 3 27 $[M-18]^-$ (MS3 327/345) of the mono-MGO adduct had the typical loss of the B-ring unit (m/z 106) (**Figure 17**) to generate the fragment ion 221 $[M-18-106]^-$ indicating that the MGO conjugated at the A-ring of phloretin (**Figure 15A**). The peak at 20.51 min had the fragment ion m/z 345$[M-72-H]^-$, which lost one MGO (m/z 72) molecule, and the MS/MS spectrum of this daughter ion (MS^3 345/417) was identical to the MS/MS spectrum of the mono-MGO adduct

(MS^2 345) (**Figures 15A** and **15B**). Therefore, the peak at 20.51 min was identified as the di-MGO adduct of phloretin. The MS3 spectrum of the most abundant daughter ion of this product (m/z 399 $[M-18]^-$) also had the fragment ion that lost the typical B-ring unit (m/z 293 $[M-18-106]^-$) (**Figure 17**), indicating that both MGO units conjugated at the A-ring, one at position 3 and the other at position 5.

When phloretin and MGO at a 1:1 ratio were incubated at 37 ºC for 1h, it was observed that the level of di-MGO adduct was higher than that from the reaction at a 3:1 ratio, both mono- and di-MGO adducts were the major products, and the amount of unreacted phloretin dramatically decreased (**Figure 12A**). At a 1:3 ratio, we found that the amount of mono-MGO adduct decreased and di-MGO adduct became the dominant product (**Figure 13A**). Increasing the amount of MGO to 100 fold of the amount of phloretin did not change the product profile in comparison to 1:3 ratio (phloretin: MGO), and there was no detectable tri-MGO adduct in this sample.

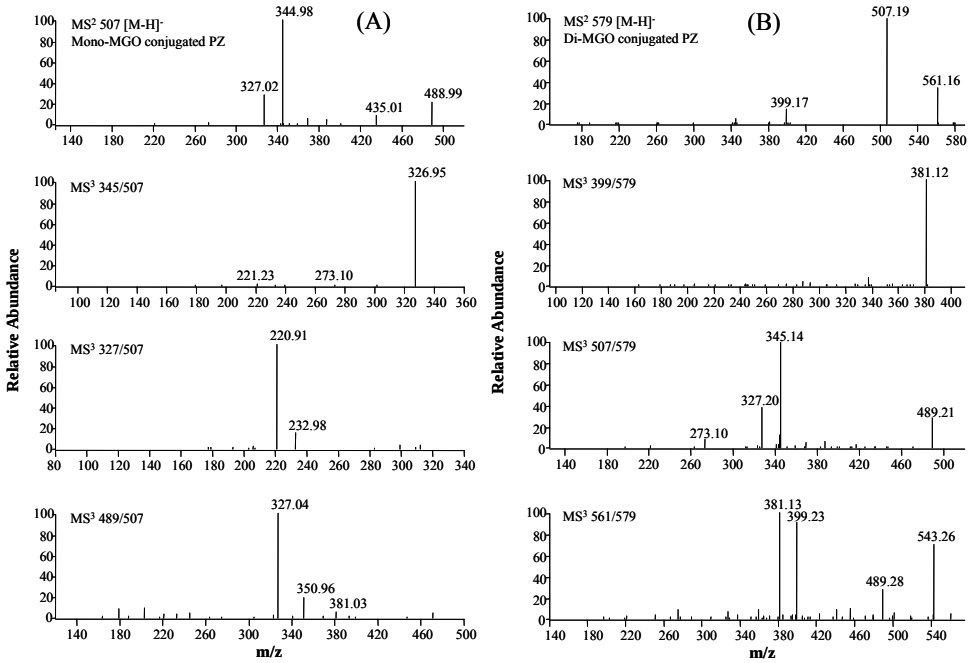

Figure 17. Tandem MS/MS spectra of (**A**) mono-MGO and (**B**) di-MGO adducts of phloridzin.

In the reaction between phloretin and GO, we found that mono-GO adduct was the major product at ratios 3:1, 1:1, and 1:3. Di-MGO adducts were not detectable in the samples from 3:1 and 1:1 reactions, and only tiny amount of di-MGO adducts were detected from the 1:3 reaction mixture after 1h incubation at 37 ºC (**Figure 13B**). At a 1:100 ratio, the amount of mono-GO adduct dramatically decreased and di-GO adducts became the dominant products (**Figure 13B**). Similar to the identification of mono-MGO adduct of phloretin, we found that the mono-GO adduct (m/z 331 $[M-H]^-$) had the fragment ion m/z 273$[M-58-H]^-$, which lost one GO (m/z 58) molecule, and the MS/MS spectrum of this daughter ion (MS^3 273/331) was identical to the MS/MS spectrum of the standard phloretin (MS^2 273) (**Figure 13A**). At a 1:100 ratio, there were two di-GO adducts formed (m/z 389 $[M-H]^-$). They had identical MS^2 spectra (data not shown) and both of them had the fragment ion m/z 331$[M-58-H]^-$, which lost one GO (m/z 58) molecule, and the MS/MS spectrum of this daughter ion (MS^3 331/389) was identical to the MS/MS spectrum of the mono-GO adduct (MS^2 331) (**Figures 16A** and **17B**). In addition, the MS3 spectrum of the most abundant daughter ion (m/z 313 $[M-18]^-$) of the mono-GO adduct (m/z 331 $[M-H]^-$) had the fragment ion m/z 207 $[M-18-106]^-$ that lost the typical B-ring unit (**Figures 16A** and **17**), and the MS/MS spectrum of the most abundant daughter ion m/z 371 $[M-18]^-$ of the di-GO adduct (MS^3 371/389) also had the typical loss of the B-ring unit to generate the fragment ion 207 $[M-18-106]^-$ (**Figures 16B** and **17**). Therefore, positions 3 and 5 at the A-ring of phloretin were also the major active sites for trapping GO.

1.3 Studying the formation of MGO and GO adducts of phloridzin by LC/MS.

Phloridzin is the mono glucoside of phloretin (**Figure 9**). In order to understand whether glucosylation affects the trapping efficacy, we conducted a similar study using phloridzin under four different ratios (3:1, 1:1, 1:3 and 1:100). We found that the trapping efficacies of phloridzin for both MGO and GO were much lower than those of phloretin, especially for short-term

reaction (**Figure 12**). Mono-MGO adduct was the major product in the reaction between phloridzin and MGO. This product was barely detectable at a 3:1 ratio after 1 h incubation of phloridzin and MGO (**Figure 14A**). The amount of this product was slightly increased at 1:1 and 1:3 ratios, and became the dominant product only at a 1:100 ratio (**Figure 14A**). Di-MGO adduct was not detectable at 3:1, 1:1, and 3:1 ratios, and only tiny amount of di-MGO adduct was formed at a 1:100 ratio (**Figure 14A**). The MS^2 spectrum of the mono-MGO adduct of phloridzin (m/z 507 $[M-H]^-$) had the fragment ion m/z 345$[M-162-H]^-$, which lost one glucose unit, and the MS/MS spectrum of this daughter ion (MS^3 345/507) was identical to the MS/MS spectrum of the mono-MGO adduct of phloretin (MS^2 345) (**Figures 15A** and **18A**), indicating that this peak was the mono-MGO adduct of phloridzin. The MS2 spectrum of the di-MGO adduct of phloridzin (m/z 579 $[M-H]^-$) had the fragment ion m/z 507[M-58-H]-, which lost one MGO (m/z 72) molecule, and the MS/MS spectrum of this daughter ion (MS^3 507/579) was identical to the MS/MS spectrum of the mono-MGO adduct (MS^2 507) (**Figures 18A** and **18B**).

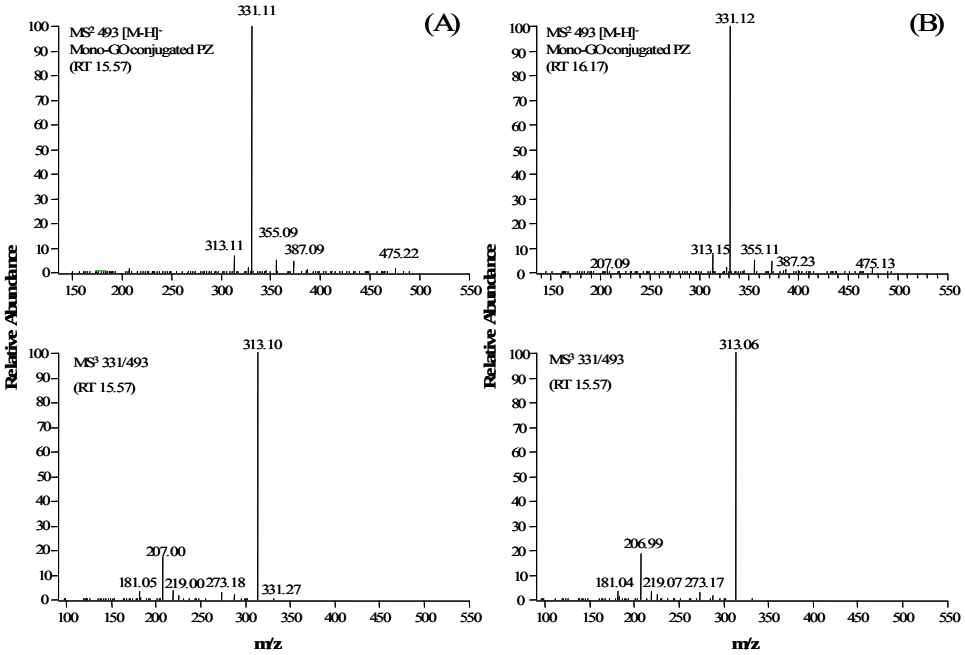

Figure 18. Tandem MS/MS spectra of mono-GO adduct of phloridzin.

In the reaction between phloridzin and GO, we found that phloridzin could not trap GO after 1 h incubation at 3:1, 1:1, and 1:3 ratios, and no product was detectable. At a 1:100 ratio, two mono-GO adducts (m/z 493 $[M-H]^-$) were formed. They had identical MS/MS spectra and both of them had the daughter ion 331 $[M-162-H]^-$, which lost one glucose unit, and the MS/MS spectrum of this daughter ion (MS^3 331/493) was identical to the MS/MS spectrum of the mono-GO adduct of phloretin (MS^2 331) (**Figures 16B** and **18**) indicating that these two products were the mono-GO adducts of phloridzin.

1.4 Purification and structure elucidation of the major mono-MGO adduct of phloridzin.

The mono-MGO adduct of phloridzin (PZMGO) was purified from the reaction between phloridzin and MGO in a 1:50 ratio using Sephadex LH-20 column eluted with ethanol. Its structure was established by analyzing the ^1H, ^{13}C, DEPT-135, and 2D NMR (1H-1H COSY, HMQC, and HMBC), as well as the MS/MS spectra. The 1D and 2D NMR spectrums of mono-PZM are shown in the appendices (**Figure 18 - 25**).

PZMGO was assigned the molecular formula $C_{24}H_{28}O_{12}$ based on negative-ion ESI-MS ($[M-H]^-$ at *m/z* 507) and the ^{13}C and DEPT-135 NMR data. The molecular weight of PZMGO was 72 (M.W. of MGO: 72) mass units higher than that of phloridzin, indicating that PZMGO was a mono-MGO adduct of phloridzin, which was further confirmed by the observation of the fragment ion *m/z* 435 $[M-H-72]^-$. Its ^1H- and ^{13}C- NMR spectra showed very similar patterns to the spectra of phloridzin (**Table 1**) [80]. The ^1H-NMR spectrum of PZMGO showed two distinct sets of aromatic ring proton signals: an AA′BB′ system for four protons, two at δ 6.64 and two at δ 7.02 (J = 8.4 Hz), indicating a para-substituted benzene ring, which was similar to those of phloridzin; and one singlet signal for one proton (δ 6.24 s), instead of the two mutually coupled doublets (2H) at δ 5.93 and δ 6.15 (J = 2.0 Hz) in the ^1H-NMR spectrum of phloridzin, suggesting MGO conjugated with phloridzin at position 3 or 5 of the A-ring. However, there were two sets

of proton signals for the MGO group (δ_H 5.32 s, 1H and 2.17 s, 3H; δ_H 3.91 m, 1H and 1.14 d, J = 6.1 Hz, 3H) instead of one set as expected in the ^{1}H NMR spectrum of PZMGO. Its ^{13}C spectra also showed two sets of carbon signals for the MGO group (δ_C 25.5 t, 71.5 d, and 206.2 s; and 24.7 t, 64.7 d, and 206.5 s). All of these features indicate that this compound is a mixture of two tautomers (**Figure 18**). In addition, in comparison with the ^{13}C spectrum of phloridzin, PZMGO had a quaternary carbon at δ_C 105.3 in its ^{13}C spectrum in lieu of an unsubstituted aromatic carbon from the A ring of phloridzin. All of these spectral features supported the presence of a MGO group in PZMGO either at the C-3 or C-5 position of the A-ring. The HMBC spectrum showed correlation between δ_C 162.2 and H-1" (δ_H 5.10 d, J = 6.8 Hz) of the glucose group indicating δ_C 162.2 was C-2 of the A-ring. In addition, the only proton on A-ring (δ_H 6.24 s) showed correlation with δ_C 162.2, suggesting that this proton was H-3 and the MGO group was located at the C-5 position of the A-ring. Thus, the structure of PZMGO was identified as shown in **Figure 18**.

Table 1. δ_H (400 MHz) and δ_C (100 MHz) NMR spectra data of phloridzin and mono-MGO conjugated phloridzin (PZMGO) (CD_3OD) (δ in ppm, J in Hz).

Position	**Phloridzin**		**PZMGO**	
	δH	δC	δH	δC
1		102.0 s		108.6
2		167.5 s		162.2
3	6.15 d, J 2.6	98.3 d	6.24 s	94.3 d
4		165.9 s		164.8
5	5.93 d, J 2.0	95.4 d		106.7 s
6		162.3 s		165.9
7		206.5 s		206.9
8	3.42 m	46.9 t	3.42 m	47
9	2.84 t, J 7.6	30.8 t	2.83 t, J 7.2	30.7
10-A			5.32 s	71.5 d
10-B				206.2 s
11-A				206.5 s
11-B			3.91 m	64.7 d
12-A			2.17 s	25.5 t

12-B			1.14 d 6.1	24.7 t
1'		133.8 s		133.7
2'	7.03 d, J 8.8	130.4 d	7.02 d, J 8.4	130.4
3'	6.66 d, J 8.8	116.0 d	6.64 d, J 8.4	116
4'		156.3 s		156.3
5'	6.66 d, J 8.8	116.0 d	6.64 d, J 8.4	116
6'	7.03 d, J 8.8	130.4 d	7.02 d, J 8.4	130.4
1"	5.10 d, J 6.8	102.0 d	5.10 d, J 6.8	102
2"	3.44 m	74.6 d	3.44 m	74.6
3"	3.42 m	78.4 d	3.42 m	78.4
4"	3.40 m	71.0 d	3.40 m	71
5"	3.42 m	78.3 d	3.42 m	78.4
6"	3.87 brd, J 12.0 3.68 dd, J 5.2, 12.0	62.3 t	3.90 brd, J 12.4 3.68 dd, J 5.6, 12.4	62.4

2. Study the structural-activity relationship for trapping dicarbonyl species by dietary flavonoids

The objective of this study was to investigate the trapping effect of naturally occurring flavonoids on MGO and GO, furthermore, the possible implications for inhibition of the formation of AGEs by quenching these two reactive dicarbonyl compounds. The trapping efficacies of flavonoids: quercetin, luteolin, epicatechin, genistein, daidzein, naringenin, and apigenin as well as their sub-components: gallic acid, pyrogallol, pyrocatechol, resorcinol, and phloroglucinol were obtained by quantifying the amounts of remaining MGO and the degrees of glycation are analyzed for the development of specific fluorescence (**Figure 26**). Seven naturally occurring flaovonids and five flavonoid sub-components were tested under *in vitro* conditions and compared within four groups.

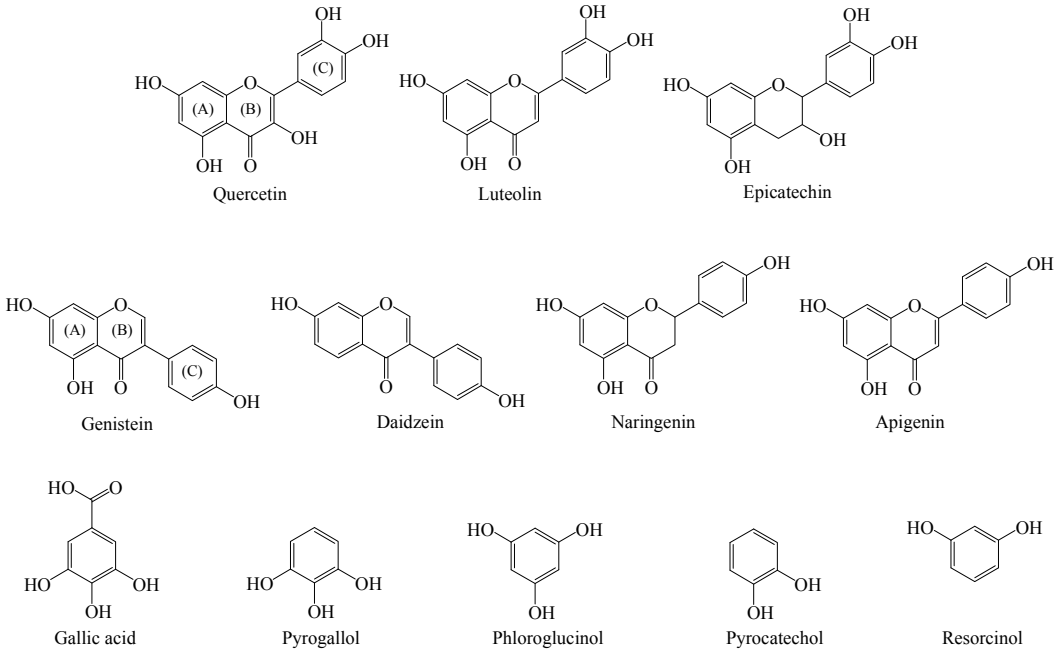

Figure 26. Chemical structures of quercetin, luteolin, epicatechin, genistein, daidzein, naringenin, apigenin, gallic acid, pyrogallol, phloroglucinol, pyrocatechol, and resorcinol.

2.1 Trapping effects of MGO by quercetin, luteolin, and epicatechin

Quercetin, luteolin, and epicatechin were selected as the first group of flavonoids due to their identical A-ring and B-ring structure but different C-ring configuration. Quercetin and luteolin belong to the flavone category with a double band between C3 and C4 and one ketone group at C4 position. Epicatechin belongs to the flavanol category with a C3-hydroxy group on the C-ring.

Quercetin shows the best trapping efficacy of MGO, followed by Luteolin, and Epicatechin. More than 90% MGO was trapped within 24hr by both quercetin and luteolin. Epicatechin also had strong trapping efficiency by quenching more than 85% MGO within 24 h (**Figure 27**). However, epicatechin shows a faster trapping speed based on the Tc 50 data. 50% of MGO was scavenged by epicatechin with 11.25 min (**Table 2**). Two conclusions were drawn based on the results of our observation on this group of flavonoids: (1) the ketone group at the C-4 position

enhances the trapping efficacy; (2) the hydroxyl group at the C-3 position could speed up the trapping reaction.

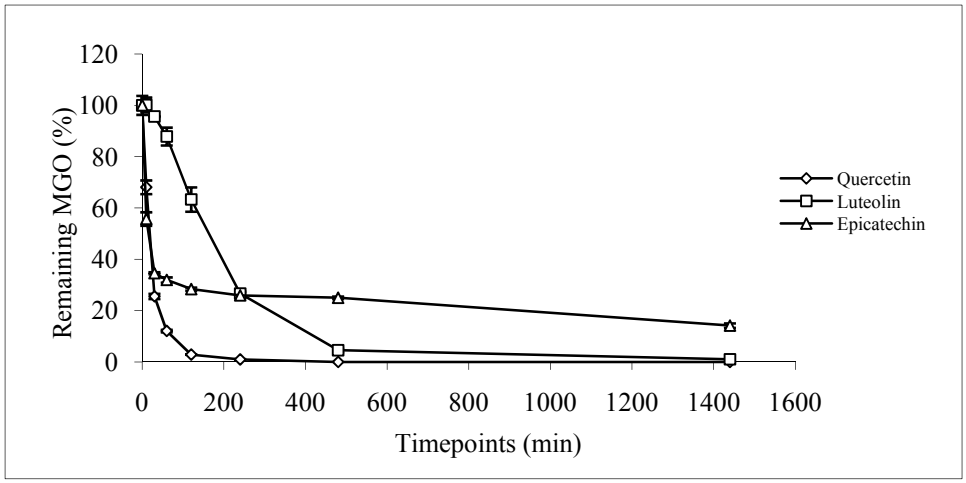

Figure 27. Trapping of MGO by quercetin, luteolin, and epicatechin in phosphate buffer (pH 7.4, 37 °C).

2.2 Trapping effects of MGO by genistein, daidzein, naringenin, and apigenin

The second group of flavonoids included: genistein, daidzein, naringenin, and apigenin. Genistein and naringenin are categorized as isoflavone. Naringenin and apigenin belong to flavanone and flavone, respectively. Genistein and naringenin have identical B-ring and C-ring configuration with different number of hydroxyl group on the A-ring. Naringenin and apigenin have the same A-ring and B-ring configuration but different C-ring structure. C2 and C3 are connected by a single-bond of naringenin, but double-bond for apigenin.

Table 2. Parameters of trapping curve of MGO by dietary flavonoids.

Compound name	IC_{50} (min)	Trapping curve equation	R^2
Phloroglucinol	928	$y = 87.23*e^{-0.0006x}$	0.8975
Pyrogallol	129	$y = 89.83*e^{-0.0045x}$	0.9075
Resorcinol	> 1440	$y = 92.705e^{-2E-04x}$	0.8632
Pyrocatechol	> 1440	$y = 96.474e^{-2E-04x}$	0.9298
Gallic acid	> 1440	$y = 96.477e^{-1E-04x}$	0.7724

Genistein	101	$y = 99.67*e^{-0.0066x}$	0.9848
Quercetin	17	$y = 100.37*e^{-0.0412x}$	0.9965
Epicatechin	11	$y = 25.25*e^{-0.0814x}$	0.9640
Luteolin	152	$y = 107.07*e^{-0.049x}$	0.9833
Apigenin	163	$y = 101.52*e^{-0.0042x}$	0.9676
Naringenin	68	$y = 103.69*e^{-0.011x}$	0.9941
Daidzein	231	$y = 101.691*e^{-0.03x}$	0.9878

In **Figure 28**, genistein showed the best trapping efficacy of MGO, followed by naringenin, Daidzein, and Apigenin. However, naringein showed the best scavenging speed of MGO among these four flavonoids. 97.69%, 96.74%, 93.89%, and 90.48% of MGO were trapped by genistein, naringenin, Daidzein, and Apigenin with 24 hr, respectively. Nevertheless, 50% of MGO was scavenged by naringenin with 67.5 min (**Table 2**). By a comparison of the structures of these four flavonoids with their trapping efficacy of MGO, three conclusions were obtained as below: (1) the connection site of B-ring on the C-ring will not significantly affect the trapping efficacy of MGO by flavnoids; (2) the hydroxyl group at the C-5 position enhances the trapping efficacy; (3) the double bond between the C-2 and C-3 positions could facilitate the trapping efficacy.

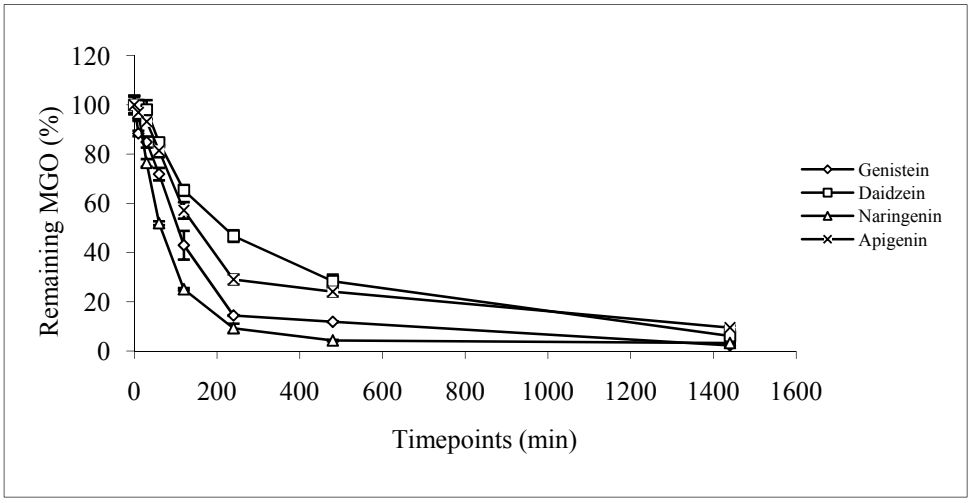

Figure 28. Trapping of MGO by genistein, daidzein, naringenin, and apigenin in phosphate buffer (pH 7.4, 37 °C).

2.3 Trapping effects of MGO by apigenin and luteolin

By comparing apigenin and luteolin (**Figure 29**), which have the same A-ring and C-ring structures but a different number of hydroxyl groups on the B-ring, we found that flavonoids have two hydroxyl groups at C-2' and C-3' position shows stronger trapping ability than those that have only one hydroxyl group on the B-ring.

2.4 Trapping effects of MGO by polyphenol sub-components: gallic acid, pyrogallol, pyrocatechol, resorinol, and phloroglucinol

As the sub-components of the flavonoids, gallic acid, pyrogallol, pyrocatechol, resorinol, and phloroglucinol were chosen as the third group (**Figure 29**). Phloroglucinol and resorcinol represent the typical A-ring of flavonoids with different number of hydroxyl groups. Pyrogallol and pyrocatechol were selected to represent the B-ring of flavonoids. Of those, pyrogallol showed the best trapping efficacy of almost 90% of MGO trapped within 24 hr incubation, followed by 60.46 % of phloroglucinol, 31.58% of resorcinol, 21.79% of pyrocatechol, and 14.86 % of gallic acid. Phloroglucinol showed the fasted trapping speed based on the Tc 50 data (**Table 2**).

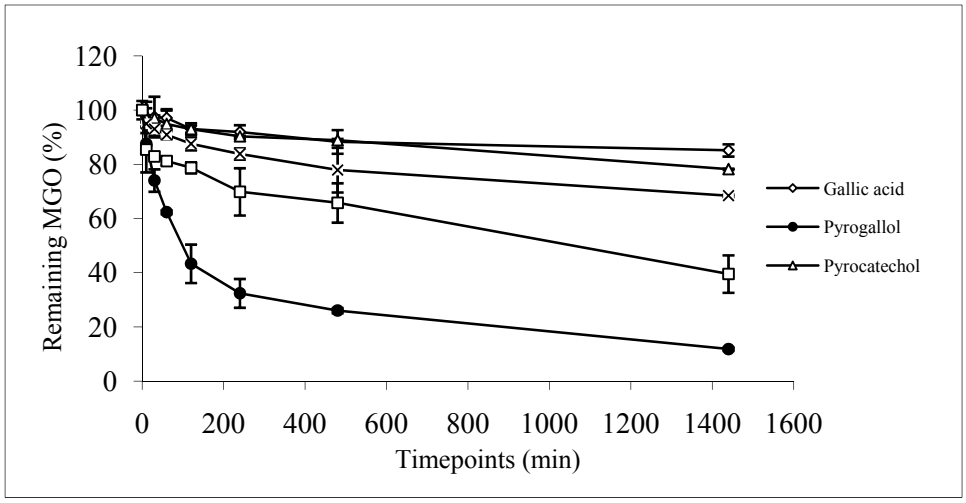

Figure 29. Trapping of MGO by gallic acid, pyrogallol, pyrocatechol, resorcinol, and phloroglucinol in phosphate buffer (pH 7.4, 37 °C).

By a comparison of the structures of these five sub-components with their trapping efficacy of MGO, the following structural requirements of flavonoids for the activity were obtained. Flavnoids with phloroglucinol as the phenolic subcomponent of the A-ring show stronger trapping effects that those with resorcinol as the A-ring subcomponent.The stronger trapping activity of pyrogallol compared to gallic acid indicates that the D-ring of flavonoids is not the active site contributing to the trapping effects. And this result further confirmed our previous conclusion obtained from EGCG-related study that the A-ring is the active site contributing the trapping activity of flavonoids.

3. Study the inhibitory effects on the formation of AGEs by dietary flavonoids

3.1 Effects of MGO on the formation of AGEs with human serum albumin

The formation of MGO-mediated protein glycation was determined by fluorescence formation. MGO readily reacts with protein residues, such as lysine and arginine, to produce high molecular weight and cross-linked adducts, which known as AGEs. The results in this study showed a dose-dependent manner of the presence of MGO with the level of AGEs in the HSA during long term incubation (**Figure 30**). The level of AGEs increased 2.2 folds and 7.4 folds in the presence of MGO with a concentration of 100 μM and 1mM, respectively.

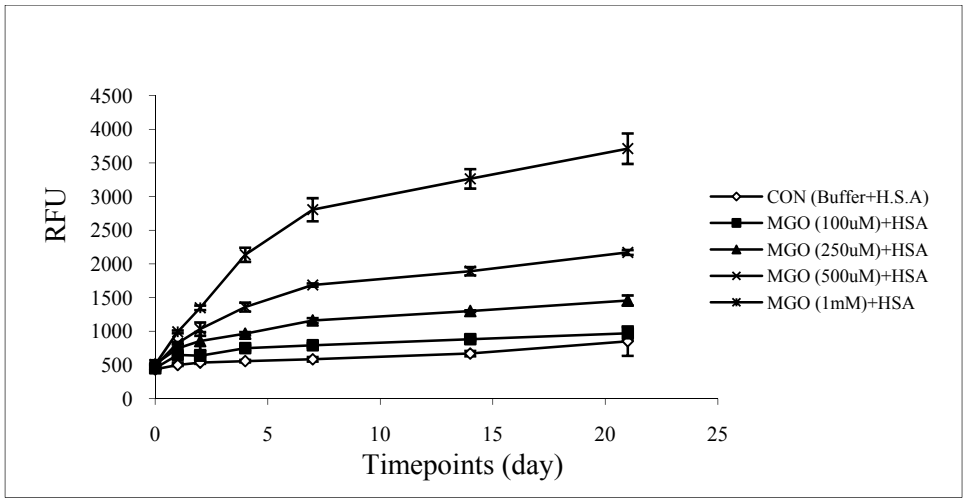

Figure 30. Formation of advanced glycation end products (AGEs) on human serum albumin (HAS) with methylglyoxal (MGO) at different concentrations (0, 100, 250, 500, and 1000 μM).

3.2 Kinetic study of the inhibitory effects on the formation of AGEs by genistein, phloretin and phloridzin

The inhibition of MGO derived AGEs was determined using fluorescence assay in the presence of three flavonoids: genistein, phloretin and phloridzin, which have shown effective trapping ability of MGO under *in vitro* condition.

In the early study, we found MGO showed significant dose-dependent manner on the formation of AGEs. However, when the genistein (1.5 mM) were present in the incubation mixture, the formation of AGEs were inhibited by almost 50%. This was an indication of protection against cross-linking by naturally occurring flavonoid through the mechanism of scavenging MGO (**Figure 31**). To further confirm our conclusion, phloretin and phloridzin were used to replace genistein as the AGEs inhibitor. These two apple derived chalcone already perform great trapping efficacy of trapping both MGO and GO in our early study. By adding these two flavonoids with different concentrations in the incubation mixtures, we observed gradually decrease on the formation of AGEs (**Figure 32** and **33**). Phloretin exhibited significant

inhibition by suppressing 45.65%, 57.91%, 67.63%, and 64.54% on the formation of AGEs at the concentration of 250, 500, 1000, and 2000 μM during long term incubation, respectively. Phloridzin also performed certain inhibition by decreasing 18.50%, 19.10%, 24.32%, and 43.98% on the formation of AGEs at the concentration of 250, 500, 1000, and 2000 μM during long term incubation, respectively. This result is consistent to our observation on the trapping efficacy of MGO and GOES by phloretin and phloridzin that phloretin exhibit stronger trapping ability of dicarbonyl species comparing to phloridzin.

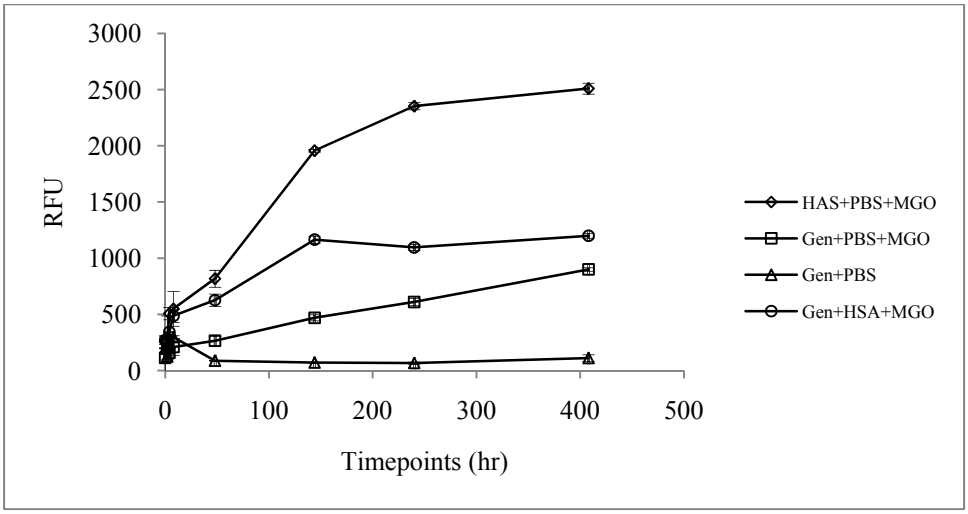

Figure 31. Inhibition of AGEs formation with genistein.

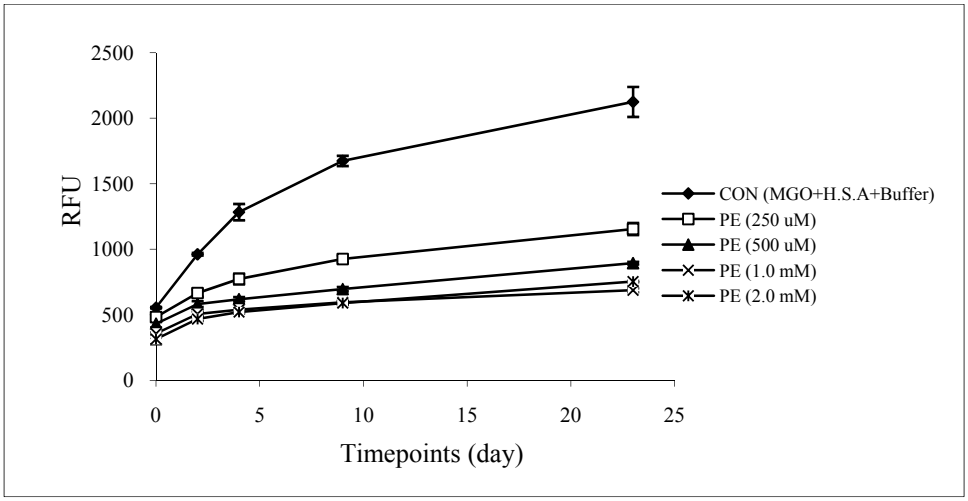

Figure 32. **.** Inhibition of AGEs formation with phloretin (PE) at different concentrations (0, 250, 500, 1000, and 2000 μM).

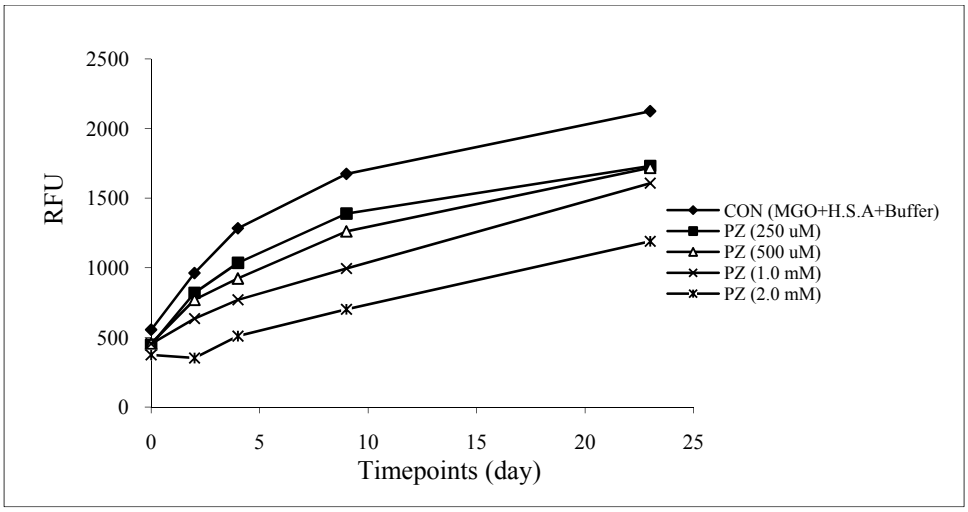

Figure 33. Inhibition of AGEs formation with phloridzin (PZ) at different concentrations (0, 250, 500, 1000, and 2000 μM).

3.3 Studying the reaction adducts of HSA, MGO, and genistein by LC/MS

The reaction mixtures of HSA with MGO in the presence of genistein were analyzed by LC/MS (**Figures 33, 34** and **35**). After 1 h incubation of genistein with MGO, two major new peaks (rt 18.48 and 19.52) appeared in the LC chromatogram. Both of these two peaks had the fragment ion m/z 343 [M-H]-, indicating that these products were the mono-MGO conjugate of genistein. When genistein and MGO were incubated at 37 ºC for longer time, it was observed that the level of mono-MGO adduct was increased. After 6 days incubation, another new peak was observed at the rt 16.24 with the molecular ion 415 [M-H]-, indicating that this was the di-MGO conjugated genistein. When the genistein (1.5 mM) was present in the incubation mixture, the formation of AGEs were inhibited by almost 50%.

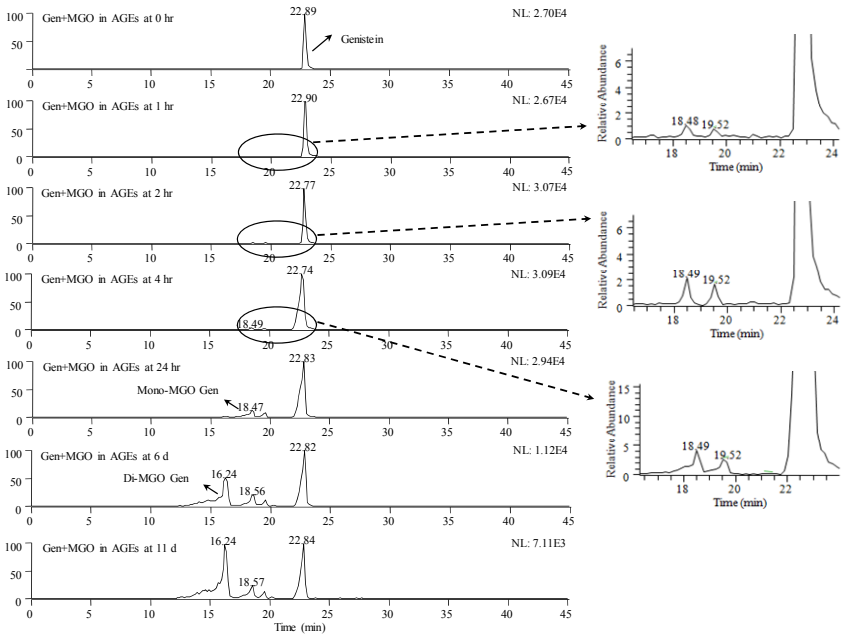

Figure 34. LC chromatograms of genistein after incubation with MGO (3:1) for 0, 1, 2, 4, 24 hr, and 11 days, respectively.

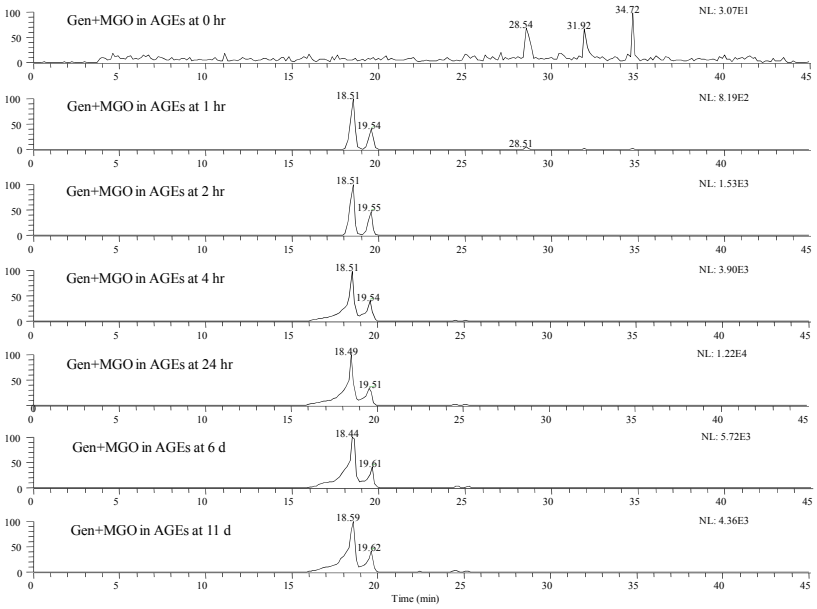

Figure 35. LC chromatograms of mono-MGO conjugated genistein (m/z 343 $[M-H]^-$) under SIM mode.

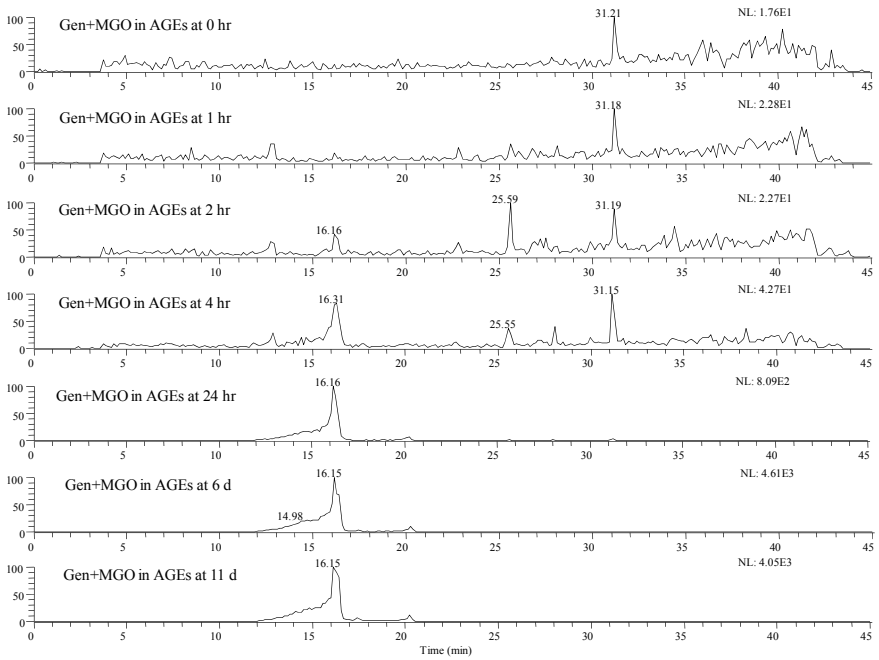

Figure 36. LC chromatograms of di-MGO conjugated genistein (m/z 415 $[M-H]^-$) under SIM mode.

SUMMARY

Increasing evidence has identified the formation of AGEs as a major pathogenic link between hyperglycemia and diabetes-related complications. In diabetes, AGEs formation occurs at a higher rate when compared to non-diabetic normal individuals. It has been well documented that AGEs progressively accumulate in the tissues and organs to develop chronic complications of diabetes mellitus. Alpha-Oxoaldehydes such as MGO and GO, the reactive dicarbonyl intermediates generated during the non-enzymatic glycation between reducing sugars and amino groups of proteins, lipids, and DNA, are precursors of AGEs and exert direct toxicity to cells and tissues. It has been shown that dicarbonyl compounds are more reactive in the glycation reaction than reducing sugars and play an important role for cross-linking proteins in the glycation process. Recent study indicated that direct administration of MGO to SD rats significantly increased the

levels of renal CEL, SBP, urinary albumin excretion, urinary thiobarbituric acid-reactive substances excretion and the renal nitrotyrosine expression in the kidney, which lead to insulin resistance and salt-sensitive hypertension. Plasma levels of MGO and GO are reportedly elevated in diabetes, dialysis, and chronic kidney disease patients. Thus decreasing the levels of MGO and GO will be a useful approach to prevent the formation of AGEs, and then prevent the development of diabetic complications.

In present study, we found that apple derived flavonoid, phloretin could rapidly trap MGO under neutral or alkaline conditions. Phloretin is a flavonoid found exclusively in apples and in apple-derived products where it is present as free and its glucosidic form, phloridzin (phloretin 2′-*O*-glucose) [80-82]. It was reported that phloridzin could be hydrolyzed to phloretin by lactase-phloridzin hydrolase in the small intestine [83]. A more recent study showed that urinary phloretin could be used as the exposure biomarker of apple consumption [84]. In addition, several studies have shown that both phloretin and phloridzin have antidiabetic effects by inhibiting intestinal glucose absorption [85, 86]. Similar to the phenomenon that we observed for EGCG, the trapping efficacy of phloretin for GO was much lower than that for MGO. This was because the hydrated monomer, dimer, and trimer were the main forms of GO in aqueous solution, and the trapping reaction between phloretin and GO was slowed down by the transformation from the hydrated monomer, dimer, and trimer to free GO. The trapping rates of phloridzin for both MGO and GO were much slower than those of phloretin, indicating the hydroxyl group at position 2 of the A ring played significant role on the trapping of reactive dicarbonyl species. In addition, our data showed that both phloretin and phloridzin were more reactive than lysine, phloretin was also more active than arginine, and phloridzin was as effective as arginine in terms of trapping MGO or GO. All of these results indicated that both phloretin and phloridzin had the potential to compete with lysine and arginine in vivo and therefore prevent the formation of AGEs.

To understand the mechanism by which phloretin and phloridzin could trap reactive dicarbonyl species, we studied the formation of MGO or GO adducts of phloretin and phloridzin using LC/MS. Our results indicated that positions 3 and 5 of the A ring of phloretin and phloridzin were the major active sites for trapping both MGO and GO. Glucosylation of the hydroxyl group at position 2 could significantly slow down the trapping rate and the formation of MGO or GO adducts. To further confirm that the A ring was the major active site; we purified the major product from the reaction between phloridzin and MGO at a 1:50 mol ratio. Its structure was identified as the PZMGO with the MGO conjugated at position 5 of the A-ring. Therefore, our results clearly indicated that the two unsubstituted carbons at the A-ring, positions 3 and 5, were the major active sites for chalcone type of compounds, which have the same A-ring as phloretin, to trap reactive dicarbonyl species. This was consistent with our previous finding that the two unsubstituted carbons at the A-ring of EGCG (positions 6 and 8 for flavanol type of compounds) were the major active sites to trap reactive dicarbonyl species and form mono- and di-MGO or GO adducts. On the basis of our observations on two different types of flavonoids, chalcone and flavanol, we predict that flavonoids that have the same A ring structure as EGCG or phloretin can efficiently trap reactive dicarbonyl species to form mono- and di-MGO or GO adducts, and glycosylation can significantly decrease the trapping efficacy. Therefore, we propose a mechanism of how flavonoids trap MGO to form mono- and di-MGO adducts. The slightly alkaline pH can increase the nucleophilicity of the unsubstituted carbons at the A ring and facilitate the addition of MGO at these two positions to form mono- and di-MGO adducts.

In order to further study the structural requirements to trap the dicarbonyl species by flavonoids. We tested seven naturally occurring flavonoids: quercetin, luteolin, epicatechin, genistein, daidzein, naringenin, apigenin as well as five flavonoid sub-components: gallic acid, pyrogallol, phloroglucinol, pyrocatechol, and resorcinol. By comparing the trapping efficacy of MGO under *in vitro* condition (37°C, pH 7.4) of these twelve compounds, we found that (1) the

connection site of B-ring on the C-ring will not significantly affect the trapping efficacy of MGO by flavnoids; (2) the hydroxyl group at the C-5 position enhances the trapping efficacy; (3) the double bond between the C-2 and C-3 positions could facilitate the trapping efficacy; (4) flavonoids have two hydroxyl groups at C-2' and C-3' position shows stronger trapping ability than those that have only one hydroxyl group on the B-ring; (5) flavnoids with phloroglucinol as the phenolic subcomponent of the A-ring show stronger trapping effects that those with resorcinol as the A-ring subcomponent. (6) The stronger trapping activity of pyrogallol compared to gallic acid indicates that the D-ring of flavonoids is not the active site contributing to the trapping effects; (7) the A-ring is the active site contributing the trapping activity of flavonoids.

To further elucidate the implication on the formation of AGEs from dicarbonyl species, the formation of MGO-mediated protein glycation was determined by fluorescence formation. The results in this study showed a dose-dependent manner of the presence of MGO with the level of AGEs in the HSA during long term incubation. Genistein, phloretin, and phloridzin were tested to inhibit the formation of AGEs through scavenging the MGO. Phloretin exhibited significant inhibition by suppressing 45.65%, 57.91%, 67.63%, and 64.54% on the formation of AGEs at the concentration of 250, 500, 1000, and 2000 μM during long term incubation, respectively. Phloridzin also performed certain inhibition by decreasing 18.50%, 19.10%, 24.32%, and 43.98% on the formation of AGEs at the concentration of 250, 500, 1000, and 2000 μM during long term incubation, respectively. These results are consistent to our observation on the trapping efficacies of MGO and GO by phloretin and phloridzin that phloretin exhibit stronger trapping ability of dicarbonyl species comparing to phloridzin.

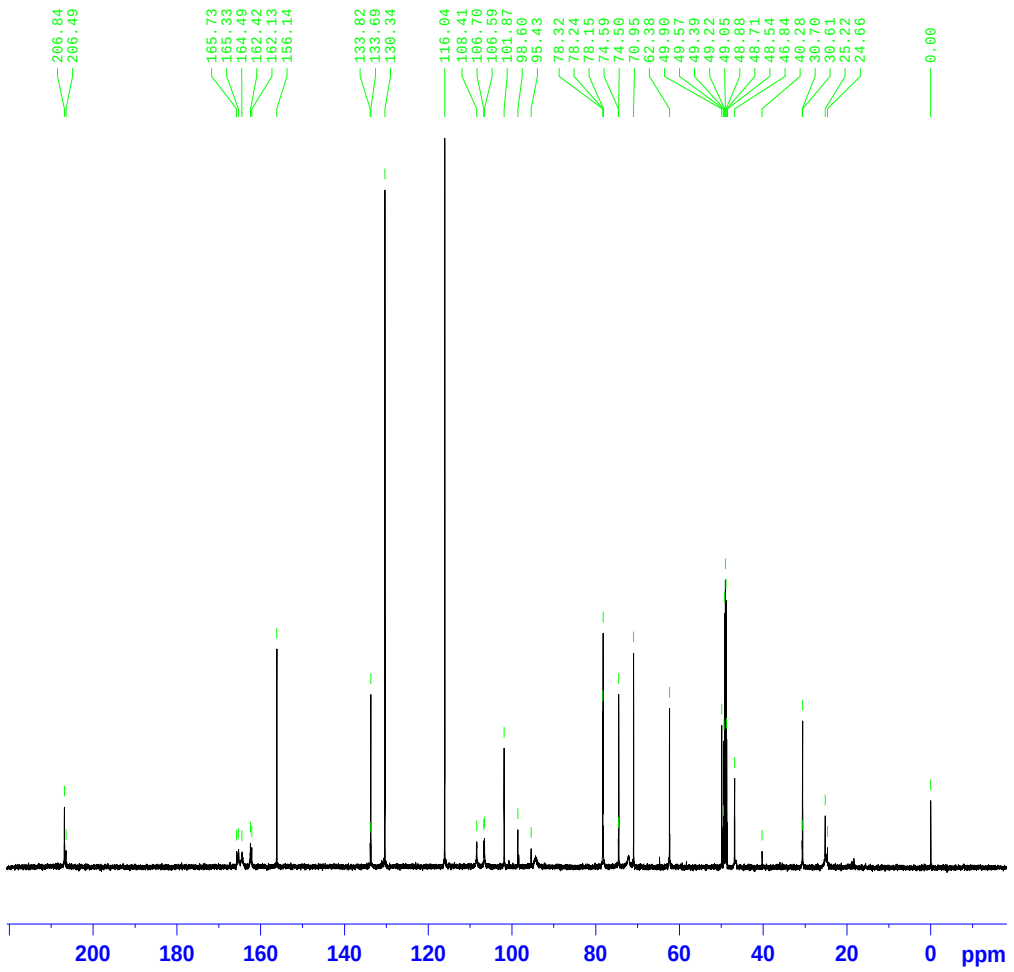

Figure 19. ^{13}C NMR spectrum of Mono-PZM at 25 ºC (CD_3OD, 125 MHz).

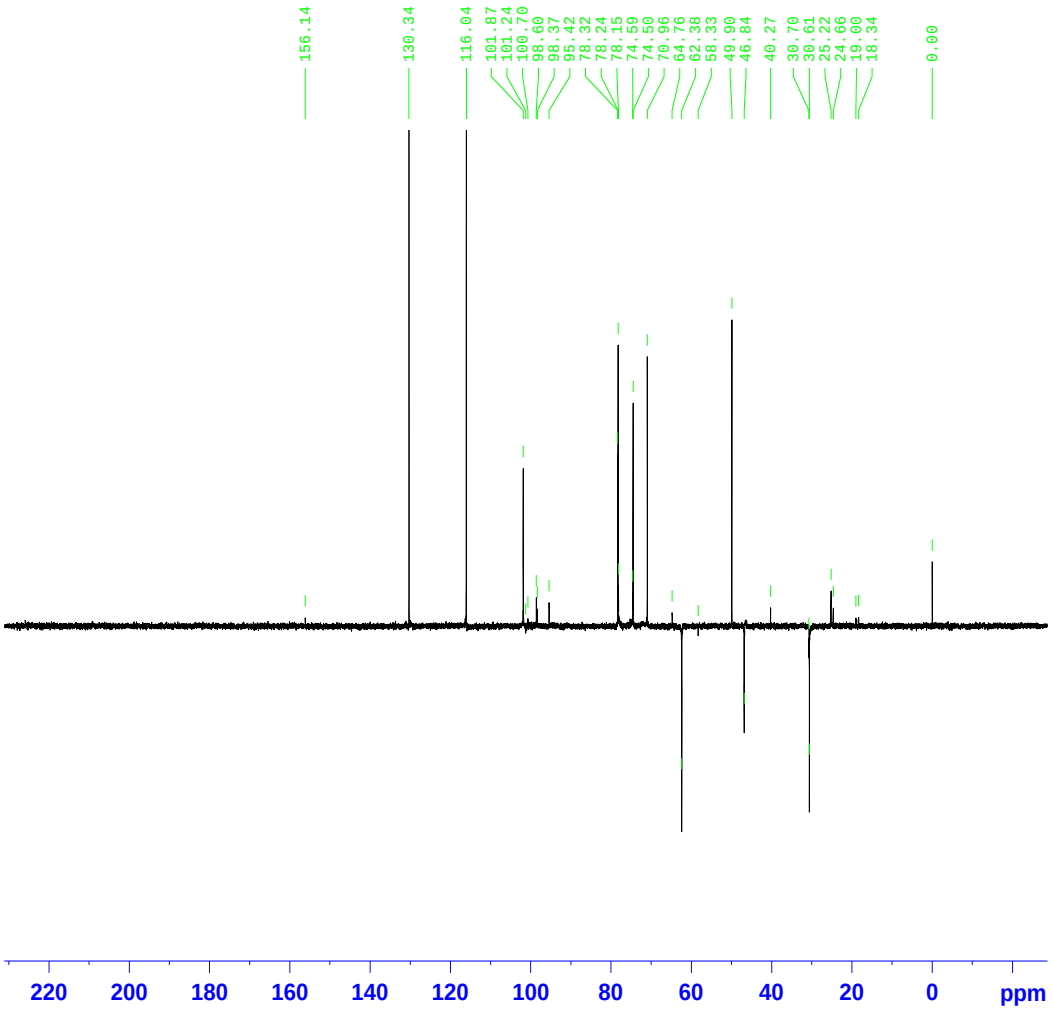

Figure 20. DEPT-135 NMR spectrum of Mono-PZM at 25 ºC (CD_3OD, 125 MHz).

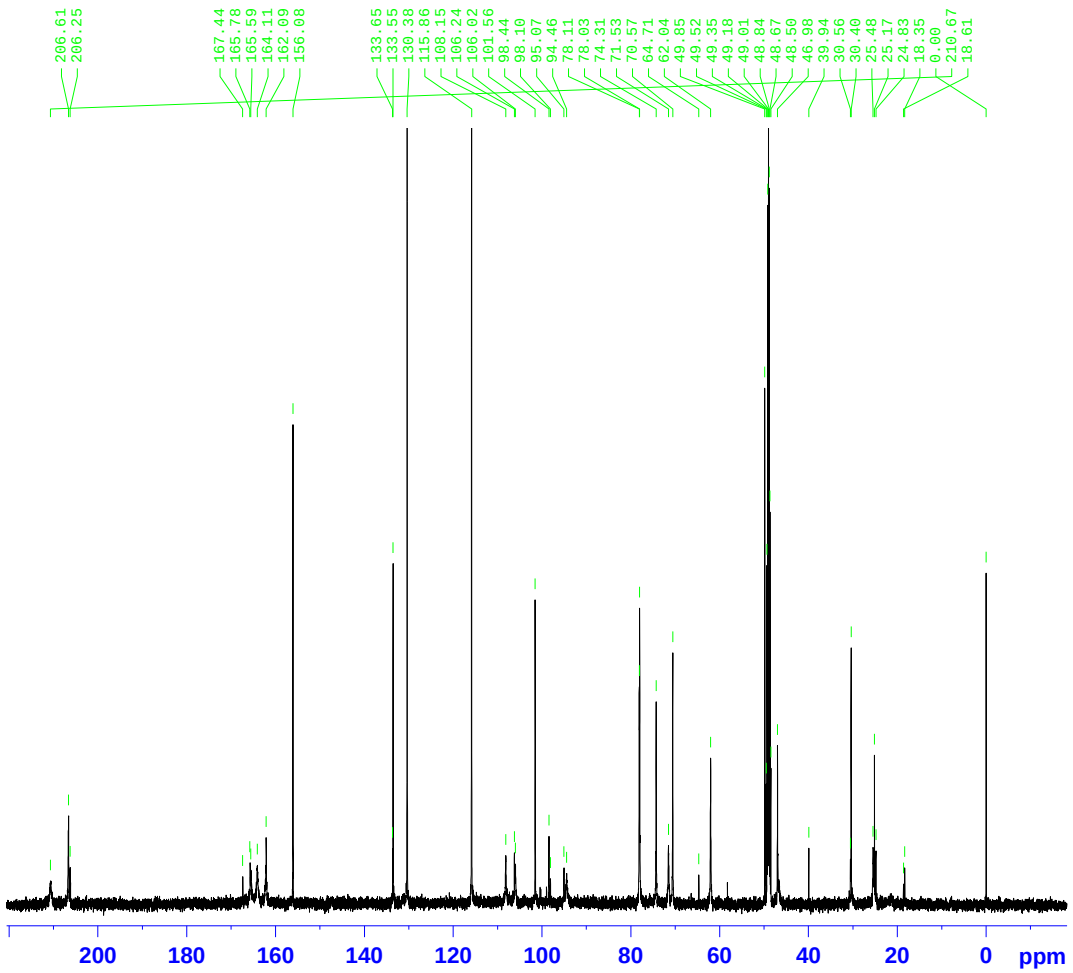

Figure 21. ^{13}C NMR spectrum of Mono-PZM at -10 ºC (CD_3OD, 125 MHz).

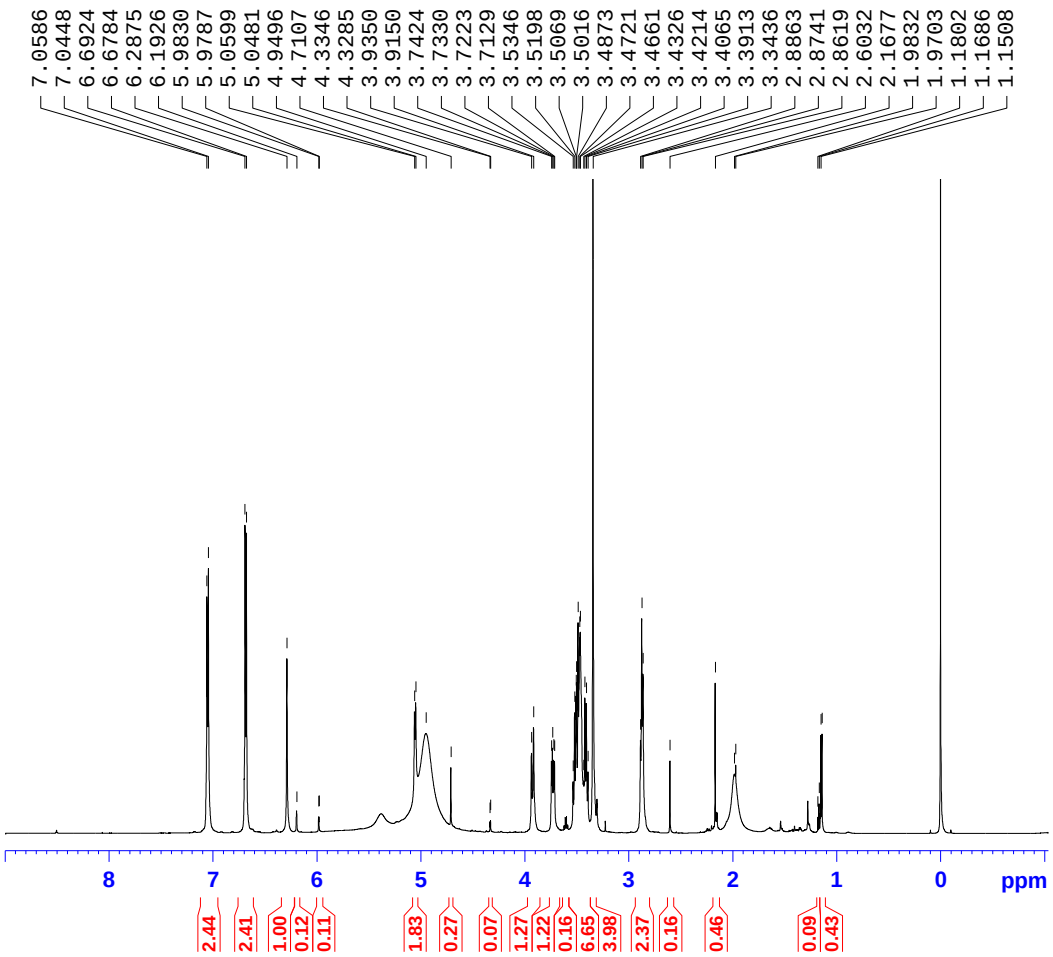

Figure 22. ^{1}H NMR spectrum of Mono-PZM at 25 ºC (CD_3OD, 600 MHz).

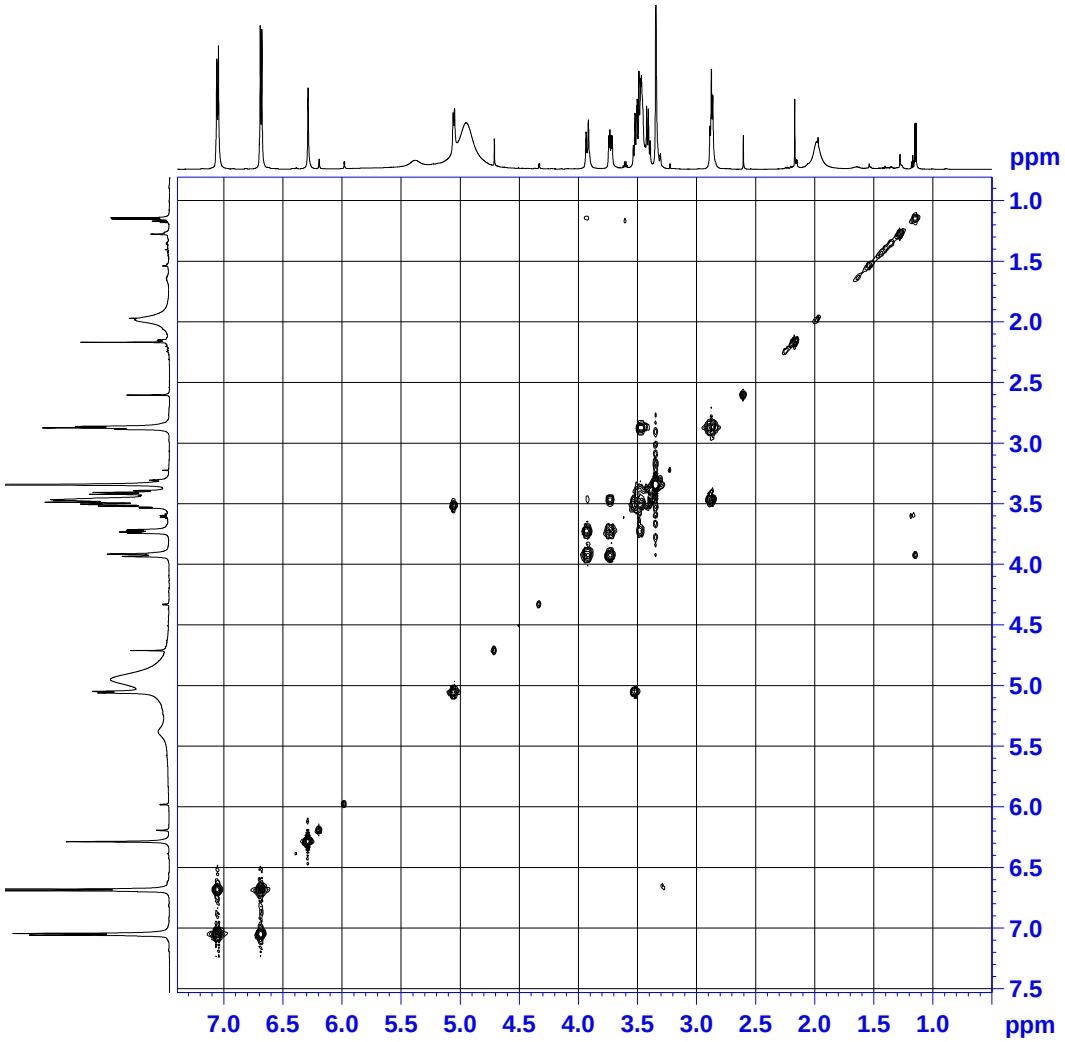

Figure 23. ^{1}H-^{1}H COSY spectrum of Mono-PZM at 25 ºC (CD_3OD, 600 MHz).

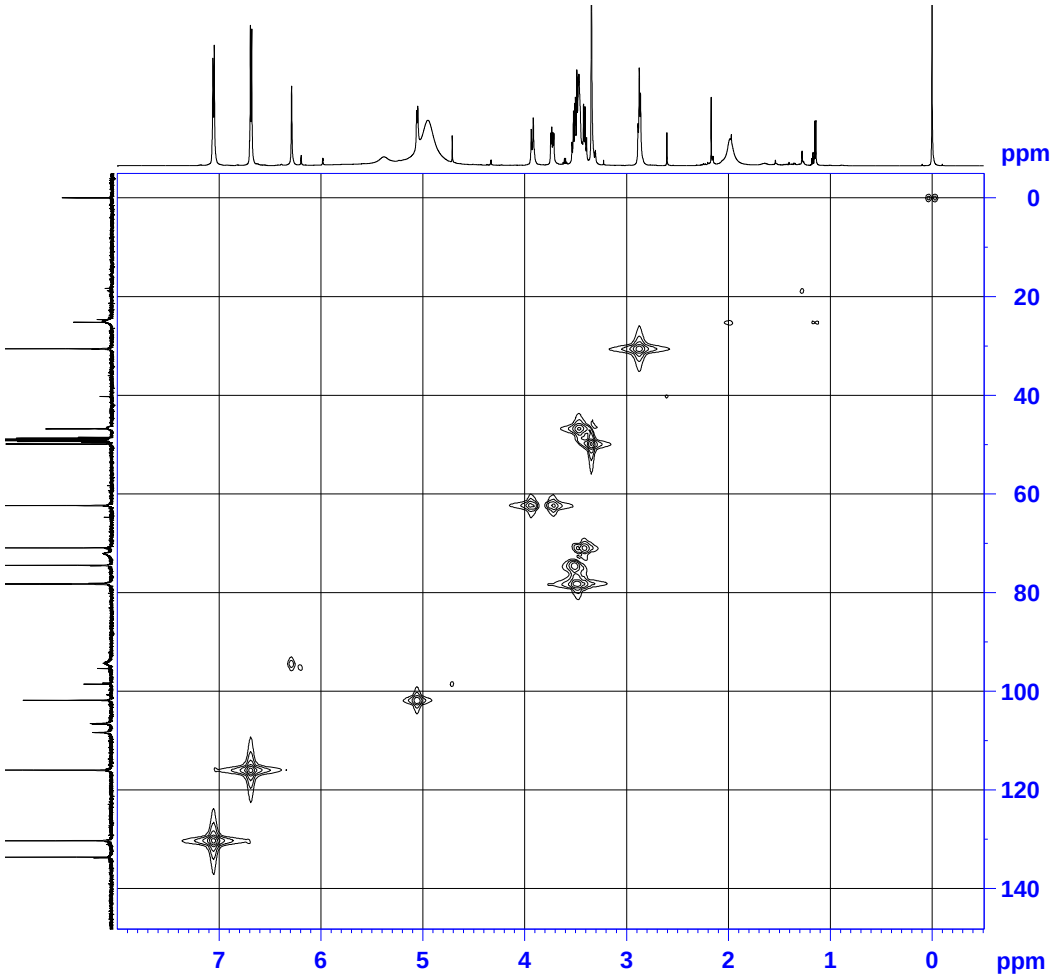

Figure 24. HMQC spectrum of Mono-PZM at 25 ºC (CD_3OD, 600 MHz).

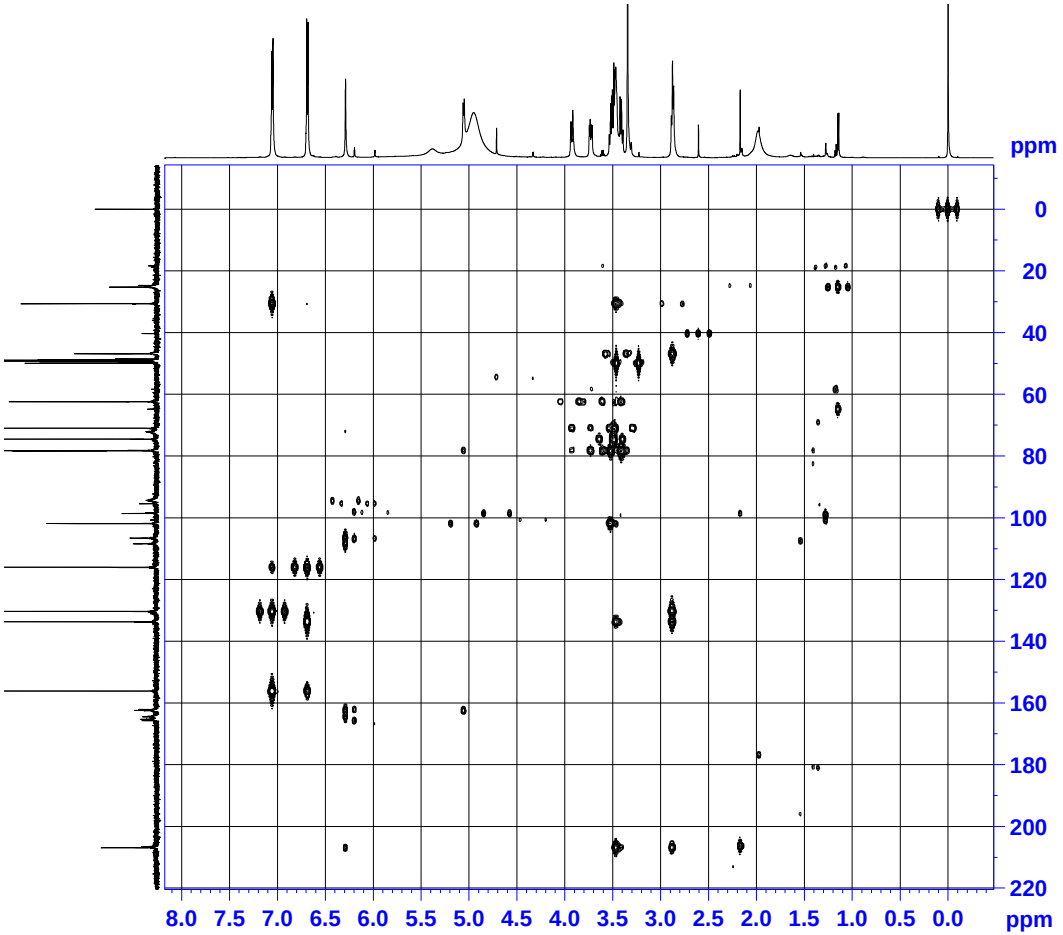

Figure 25. HMBC spectrum of Mono-PZM at 25 ºC (CD_3OD, 600 MHz).

REFERENCES

[1] Beisswenger, P. J.; Szwergold, B. S. α-Oxoaldehyde metabolism and diabetic complications. *Biochemical Society Transactions* **2003**, 31, 1358-1363.

[2] Nemet, I.; Varga-Defterdarovi, L.; Turk, Z. Methylgloxal in food and living organisms. *Molecular Nutrition & Food Research* **2006**, 50, (12), 1105-1117.

[3] Arribas-lorenzo, G.; Morales, F. J. Analysis, Distribution, and Dietary Exposure of Glyoxal and Methylglyoxal in Cookies and Their Relationship with Other Heat-Induced Contaminants. *Journal of Agriculture and Food Chemistry* **2010**, 58, (5), 2966-2972.

[4] Nagao, M.; Fujita, Y.; Sugimura, T.; Kosuge, T. Methylglyoxal in beverages and foods: its mutagenicity and carcinogenicity. *IARC scientific publications* **1986**, 70, 283-291.

[5] Roiter, I. M.; Borovikova, L. A. Level of volatile carbonyl compounds in bread during the addition of enzyme preparations. *Khlebopek. Konditer. Promst* **1972**, 14, 14-15.

[6] Wells-Knecht, K. J.; Zyzak, D. V.; Litchfield, J. E.; Thorpe, S. R.; Baynes, J. W. Mechanism of autoxidative glycosylation: identification of glyoxal and arabinose as intermediates in the autoxidative modification of proteins by glucose. *Biochemistry* **1995**, 34, (11), 3702-3709.

[7] Wittmann, R.; Eichner, K. Detection of Maillard products in malts, beers, and brewing couleurs. *Z. Lebensm.-Unters.-Forsch* **1989**, 188, 212-220.

[8] Adriana, B.; Beatriz, S.; Erika, S.; Julio, H.; Rafael, R.-A. α-Dicarbonylic compounds as indicators and precursors of flavor deterioration during beer aging. *Technical quarterly - Master Brewers Association of the Americas* **2002**, 39, (1), 13-23.

[9] Bravo, A.; Herrera, J. C.; Scherer, E.; Ju-Nam, Y.; Rubsam, H.; Madrid, J.; Zufall, C.; Rangel-Aldao, R. Formation of r-Dicarbonyl Compounds in Beer during Storage of Pilsner. *Journal of Agriculture and Food Chemistry* **2008**, 56, (11), 4134-4144.

[10] Revel, G. D.; Bertrand, A., Dicarbonyl compounds and their reduction products in wine, Identification of wine aldehydes. In *Proc 7th Weurman Flavour Research Symp*, Zeist, 1994; pp 353-361.

[11] Revel, G. D.; Pripis-Nicolau, L.; Barbe, J. C.; Bertrand, A. The detection of α-dicarbonyl compounds in wine by formation of quinoxaline derivatives. *Journal of the Science of Food and Agriculture* **2000**, 80, 102-108.

[12] Hayashi, T.; Shibamoto, T. Analysis of Methyl Glyoxal in Foods and Beverages. *Journal of Agriculture and Food Chemistry* **1985**, 33, (6), 1090-1093.

[13] Daglia, M.; Papetti, A.; Aceti, C.; Sordelli, B.; Spini, V.; Gazzani, G. Isolation and Determination of r-Dicarbonyl Compounds by RP-HPLC-DAD in Green and Roasted Coffee. *Journal of Agriculture and Food Chemistry* **2007**, 55, (22), 8877-8882.

[14] Marshall, R. O.; Kooi, E. R. Enzymatic conversion of D-glucose to D-fructose. *Science* **1957**, 125, (3249), 648-649.

[15] Lo, C.-Y.; Li, S.; Wang, Y.; Tan, D.; Pan, M.-H.; Sang, S.; Ho, C.-T. Reactive dicarbonyl compounds and 5-(hydroxymethyl)-2-furfural in carbonated beverages containing high fructose corn syrup. *Food Chemistry* **2008**, 107, (3), 1099-1105.

[16] Tan, D.; Wang, Y.; Lo, C.-y.; Sang, S.; Ho, C.-t. Methylglyoxal: Its Presence in Beveragesand Potential Scavengers. *Annals of the New York Academy of Sciences* **2008**, 1126, (1), 72-75.

[17] Weigel, K. U.; Opitz, T.; Henle, T. Studies on the occurrence and formation of 1,2-dicarbonyls in honey. *European Food Research and Technology* **2004**, 218, (2), 147-151.

[18] Mavric, E.; Wittmann, S.; Barth, G.; Henle, T. Identification and quantification of methylglyoxal as the dominant antibacterial constituent of Manuka(Leptospermum scoparium) honeys from New Zealand. *Molecular nutrition & food research* **2008**, 52, (4), 483-489.

[19] Halliwell, B.; Chirico, S. Lipid peroxidation: its mechanism, measurement, and significance. *The American Journal of Clinical Nutrition* **1993**, 57, 715-724.

[20] Fujioka, K.; Shibamoto, T. Formation of genotoxic dicarbonyl compounds in dietary oils upon oxidation. *Lipids* **2004**, 39, (5), 481-486.

[21] Lyles, G. A.; Chalmers, J. The metabolism of aminoacetone to methylglyoxal by semicarbazide-sensitive amine oxidase in human umbilical artery. *Biochemical Pharmacology* **1992**, 43, (7), 1409-1414.

[22] Casazza, J. P.; Felver, M. E.; Veech, R. L. The Metabolism of Acetone in Rat. *The Journal of Biological Chemistry* **1984**, 259, (1), 231-236.

[23] Kalapos, M. P. Methylglyoxal in living organisms: Chemistry, biochemistry, toxicologyl and biological implications. *Toxicology letters* **1999**, 110, (3), 145-175.

[24] Pompliano, D. L.; Peyman, A.; Knowles, J. R. Stabilization of a reaction intermediate as a catalytic device: definition of the functional role of the flexible loop in triosephosphate isomerase. *Biochemistry* **1990**, 29, (13), 3186-3194.

[25] Richard, J. P. Mechanism for the formation of methylglyoxal from triosephosphates. *Biochemical Society transactions* **1993**, 21, (2), 549-53.

[26] Singh, R.; Barden, A.; Mori, T.; Beilin, L. Advanced glyxation end-products: a review. *Diabetologia* **2001**, 42, (2), 129-146.

[27] Miyata, T.; Ueda, Y.; Shinzato, T.; Iida, Y.; Tanaka, S.; Kurokawa, K.; Strihou, C. v. Y. d.; Maeda, K. Accumulation of albumin-linked and free-form pentosidine in the circulation of uremic patients with end-stage renal failure: renal implications in the pathophysiology of pentosidine. *Journal of the American Society of Nephrology* **1996**, 7, 1198-1206.

[28] Golej, J.; Hoeger, H.; Radner, W.; Unfried, G.; Lubec, G. Oral administration of methylglyoxal leads to kidney collagen accumulation in the mouse. *Life Sci* **1998**, 63, (9), 801-807.

[29] Guo, Q.; Mori, T.; Jiang, Y.; Osaki, Y.; Yoneki, Y.; Ogawa, S.; Miyata, T.; Ito, S. Methylglyoxal (MG) Contributes to the Development of Insulin Resistance and Salt Sensitivity in

Sprague Dawley (SD) Rats. *Journal of Hypertension* **2009**, 27, (8), 1664-1671.

[30] Guha, M. K.; Vander Jagt, D. L.; Creighton, D. J. Diffusion-dependent rates for the hydrolysis reaction catalyzed by glyoxalase II from rat erythrocytes. *Biochemistry* **1988**, 27, (24), 8818-8822.

[31] Barrenscheen, H. K.; Braun, K. Farb-und Fallungsreaktionen des Methylglyoxals. *Biocheniische Zeitschrift* **1931**, 233, 296-304.

[32] Roberts, M. J.; Wondrak, G. T.; Laurean, D. C.; Jacobson, M. K.; Jacobson, E. L. DNA damage by carbonyl stress in human skin cells *Mutation Research/Fundamental and Molecular Mechanisms of Mutagenesis* **2003**, 522, (1-2), 45-56.

[33] DeGrootb, J.; Verzijlb, N.; Budde, M.; Bijlsma, J. W. J.; Lafeber, F. P. J. G.; TeKoppele, J. M. Accumulation of Advanced Glycation End Products Decreases Collagen Turnover by Bovine Chondrocytes. *Experimental Cell Research* **2001**, 266, (2), 303-310.

[34] Jakus, V.; Rietbrock, N. Advanced glycation end-products and the progress of diabetic vascular complications. *Physiological research* **2004**, 53, (2), 131-142.

[35] Gugliucci, A. Glycation as the glucose link to diabetic complications. *Clinical practice* **2000**, 100, (10), 621-634.

[36] Odani, H.; Shinzato, T.; Matsumoto, Y.; Usami, J.; Maeda, K. Increase in three alpha, beta-dicarbonyl compound levels in human uremic plasma: specific in vivo determination of intermediates in advanced Maillard reaction. *Biochemical and Biophysical Research Communications* **1999**, 256, (1), 89-93.

[37] Nagaraj, R. H.; Sarkara, P.; Mallya, A.; Biemelc, K. M.; Ledererc, M. O.; Padayattia, P. S. Effect of pyridoxamine on chemical modification of proteins by carbonyls in diabetic rats: characterization of a major products from the reaction of pyridoxamine and methylglyoxal. *Archives of Biochemistry and Biophysics* **2002**, 402, (1), 110-119.

[38] Brunner, N. A.; Brinkmann, H.; Siebers, B.; Hensel, R. NAD1-dependent Glyceraldehyde-3-phosphate Dehydrogenase from Thermoproteus tenax. *The Journal of Biological Chemistry* **1998**, 279, (11), 6149–6156.

[39] Lederer, M. O.; Klaiber, R. G. Cross-linking of proteins by Maillard processes: characterization and detection of lysine-arginine cross-links derived from glyoxal and methylglyoxal. *Bioorganic & Medicinal Chemistry* **1999**, 7, (11), 2499-2507.

[40] Paul, R. G.; Avery, N. C.; Slatter, D. A.; Sims, T. J.; Bailey, A. J. Isolation and characterization of advanced glycation end products derived from the in vitro reaction of ribose and collagen. *The Biochemical journal* **1998**, 330, 1241-1248.

[41] Hakim, I. A.; Alsaif, M. A.; Alduwaihy, M.; Al-Rubeaan, K.; Al-Nuaim, A. R.; Al-Attas, O. S. Tea consumption and the prevalence of coronary heart disease in Saudi adults: results from a Saudi national study. *Preventive Medicine* **2003**, 36, (1), 64-70.

[42] Bucala, R.; Vlassara, H. Advanced Glycosylation Endproducts in Diabetic Renal Disease: Clinical Measurement, Pathophysiological Significance, and Prospects for Pharmacological

Inhibition. *Blood Purification* **1995**, 13, (3-4), 160-170.

[43] Bucala, R.; Vlassara, H. Advanced glycosylation end products in diabetic renal and vascular disease. *American journal of kidney diseases* **1995**, 26, (6), 875-888.

[44] Boltona, W. K.; Cattranb, D. C.; Williamsc, M. E.; Adlerd, S. G.; Appele, G. B.; Cartwrightf, K.; Foilesf, P. G.; Freedmang, B. I.; Raskinh, P.; Ratner, R. E.; Spinowitzk, B. S.; Whittierl, F. C.; Wuerth, J.-P. Randomized Trial of an Inhibitor of Formation of Advanced Glycation End Products in Diabetic Nephropathy. *American Journal of Nephrology* **2004**, 24, (1), 32-40.

[45] Lo, T. W.; Selwood, T.; Thornalley, P. J. The reaction of methylglyoxal with aminoguanidine under physiological conditions and prevention of methylglyoxal binding to plasma proteins. *Biochemical pharmacology* **1994**, 48, (10), 1865-1870.

[46] Edelstein, D.; Brownlee, M. Mechanistic studies of advanced glycosylation end product inhibition by aminoguanidine. *Diabetes* **1992**, 41, (1), 26-29.

[47] Stadler, K.; Jenei, V.; Somogyi, A.; Jakus, J. Beneficial effects of aminoguanidine on the cardiovascular system of diabetic rats. *Diabetes/metabolism research and reviews* **2005**, 21, (2), 189-196.

[48] Beisswenger, P.; Ruggiero-Lopez, D. Metformin inhibition of glycation processes. *Diabetes & Metabolism* **2003**, 29, (4), 95-103.

[49] Yang, C. S.; Lee, M. J.; Chen, L.; Yang, G. Y. Polyphenols as Inhibitors of Carcinogenesis. *Environmental Health Perspectives* **1997**, 105, (4), 971-976.

[50] Knekt, P.; Kumpulainen, J.; Jarvinen, R.; Rissanen, H.; Heliovaara, M.; Reunanen, A.; Hakulinen, T.; Aromaa, A. Flavonoid intake and risk of chronic diseases. *The American journal of clinical nutrition* **2002**, 76, (3), 560-568.

[51] Tsuneki, H.; Ishizuka, M.; Terasawa, M.; Wu, J. B.; Sasaoka, T.; Kimura, I. Effect of green tea on blood glucose levels and serum proteomic patterns in diabetic (db/db) mice and on glucose metabolism in healthy humans. *BMC Pharmacology* **2004**, 4, 18.

[52] Hosoda, K.; Wang, M.-F.; Liao, M.-L.; Chuang, C.-K.; Iha, M.; Clevidence, B.; Yamamoto, S. Antihyperglycemic effect of oolong tea in type 2 diabetes. *Diabetes Care* **2003**, 26, (6), 1714-1718.

[53] Matsumoto, N.; Ishigaki, F.; Ishigaki, A.; Iwashina, H.; Hara, Y. Reduction of Blood Glucose Levels by Tea Catechin. *Bioscience, biotechnology, and biochemistry* **1993**, 57, (4), 525-527.

[54] Choi, J. S.; Yokozawa, T.; Oura, H. Improvement of hyperglycemia and hyperlipemia in streptozotocin-diabetic rats by a methanolic extract of Prunus davidiana stems and its main component, prunin. *Planta medica* **1991**, 57, (3), 208-211.

[55] Matsui, T.; Ebuchi, S.; Kobayashi, M.; Fukui, K.; Sugita, K.; Terahara, N.; Matsumoto, K. Anti-hyperglycemic effect of diacylated anthocyanin derived from Ipomoea batatas cultivar Ayamurasaki can be achieved through the alpha-glucosidase inhibitory action. *Journal of agricultural and food chemistry* **2002**, 50, (25), 7244-7248.

[56] Vessal, M.; Hemmati, M.; Vasei, M. Antidiabetic effects of quercetin in streptozocin-induced diabetic rats. *Comparative biochemistry and physiology. Toxicology & pharmacology* **2003**, 135C, (3), 357-364.

[57] Lee, J. S. Effects of soy protein and genistein on blood glucose, antioxidant enzyme activities, and lipid profile in streptozotocin-induced diabetic rats. *Life Science* **2006**, 79, (16), 1578-1584.

[58] Hase, M.; Babazono, T.; Information, C.; Karibe, S.; Kinae, N.; Iwamoto, Y. Renoprotective effects of tea catechin in streptozotocin- induced diabetic rats. *International Urology and Nephrology* **2006**, 38, (3-4), 693-699.

[59] Yamabe, N.; Yokozawa, T.; Oya, T.; Kim, M. Therapeutic potential of (-)-epigallocatechin 3-O-gallate on renal damage in diabetic nephropathy model rats. *The Journal of pharmacology and experimental therapeutics* **2006**, 39, (1), 228-236.

[60] Rutter, K.; Sell, D. R.; Fraser, N.; Obrenovich, M.; Zito, M.; Starke-Reed, P.; Monnier, V. M. Green tea extract suppresses the age-related increase in collagen crosslinking and fluorescent products in C57BL/6 mice. *International journal for vitamin and nutrition research* **2003**, 73, (6), 453-460.

[61] Ping, O. Y.; Peng, W. L.; Xu, D. L.; W.Y. Lai; Xu, A. L. Green tea polyphenols inhibit advanced glycation end product-induced rat vascular smooth muscle cell proliferation. *Di Yi Jun Yi Da Xue Xue Bao* **2004**, 24, (3), 247-251.

[62] Chaplen, F. W. R.; Fahl, W. E.; Cameron, D. C. Method for Determination of Free Intracellular and Extracellular Methylglyoxal in Animal Cells Grown in Culture. *Analytical Biochemistry* **1996**, 238, (1), 171-178.

[63] McLellan, A. C.; Phillips, S. A.; Thornalley, P. J. Fluorometric assay of D-lactate. *Analytical Biochemistry* **1992**, 206, (1), 12-16.

[64] Nemet, I.; Varga-Defterdarovi, L.; Turk, Z. Preparation and quantification of methylglyoxal in human plasma using reverse-phase high-performance liquid chromatography. *Clinical Biochemistry* **2004**, 37, (10), 875-881.

[65] Espinosa-Mansilla, A.; Duran-Meras, I.; Salinas, F. High-performance liquid chromatographic-fluorometric determination of glyoxal, methylglyoxal, and diacetyl in urine by prederivatization to pteridinic rings. *Analytical Biochemistry* **1998**, 255, (2), 263-273.

[66] Randella, E. W.; Vasdevb, S.; Gillb, V. Measurement of methylglyoxal in rat tissues by electrospray ionization mass spectrometry and liquid chromatograhy. *Journal of Pharmacological and Toxicological Methods* **2005**, 51, (2), 153-157.

[67] Lapolla, A.; Flamini, R.; Vedova, A. D.; Senesi, A.; Reitano, R.; Fedele, D.; Basso, E.; Seraglia, R.; Traldi, P. Glyoxal and Methylglyoxal Levels in Diabetic Patients: Quantitative Determination by a New GC/MS Method. *Clinical Chemistry and Laboratory Medicine* **2003**, 41, (9), 1166–1173.

[68] Sell, D. R.; Monnier, V. M. End stage renal disease and diabetes catalyse the formation of a pentose-derived cross-link form aging human collagen. *The Journal of Clinical Investigation*

1990, 85, 380-384.

[69] Nagai, P.; Araki, T.; Hayashi, C. M.; hayase, F.; Horiuchi, S. Identification of Nε -(Carboxymethyl)Lysine, one of the methylglyoxal-derived AGE structures, in glucose-modified protein: mechanism for protein modification by reactive aldehydes. *Journal of Chromatography B* **2005**, 788, 75-84.

[70] Makita, Z.; Yanagisawa, K.; Kuwajima, S.; Bucala, R.; Vlassara, H.; Koike, T. The role of advanced glycosylation end-products in the pathogenesis of atherosclerosis. *Nephrol Dial Transplant* **1996**, 11, 31-33.

[71] Münch, G.; Keis, R.; Weßels, A.; Riederer, P.; Bahner, U.; Heidland, A.; Niwa, T.; Lemke, H.-D.; Schinzel, R. Determination of Advanced Glycation End Products in Serum by Fluorescence Spectroscopy and Competitive ELISA. *Clinical Chemistry and Laboratory Medicine* **1997**, 35, (9), 669–678.

[72] Soulis, T.; Thallas, V.; Youssef, S.; Gilbert, R. E.; McWilliam, B. G.; Murray-McIntosh, R. P.; Cooper, M. E. Advanced glycation end-products and their receptors co-localise in rat organs susceptible to diabetic microvascular injury. *Diabetologia* **1997**, 40, (6), 619-628.

[73] Ikeda, K.; Higashi, T.; Sano, H.; Jinnouchi, Y.; Yoshida, M.; Araki, T.; Ueda, S.; Horiuchi, S. N (epsilon)-(carboxymethyl)lysine protein adduct is a major immunological epitope in proteins modified with advanced glycation end products of the Maillard reaction. *Biochemistry* **1996**, 35, (24), 8075-8083.

[74] Lapolla, A.; Fedele, D.; Reitano, R.; Aricò, N. C.; Seraglia, R.; Traldi, P.; Marotta, E.; Tonani, R. Enzymatic digestion and mass spectrometry in the study of advanced glycation end products/peptides. *Journal of the American Society for Mass Spectrometry* **2004**, 15, (4), 496-509.

[75] Hilt, P.; Schieber, A.; Yildirim, C.; Arnold, G.; Klaiber, I.; Conrad, J.; Beifuss, U.; Carle, R. Detection of phloridzin in strawberries (Fragaria x ananassa Duch.) by HPLC-PDA-MS/MS and NMR spectroscopy. *Journal of Agriculture and Food Chemistry* **2003**, 51, (10), 2896-2899.

[76] Gonzalez-reche, L. M.; Kucharczyk, A.; Musiol, A. K.; Kraus, T. Determination of Nε-(carboxymethyl)lysine in exhaled breath condensate using isotope dilution liquid chromatography/electrospray ionization tandem mass spectrometry. *Rapid communications in mass spectrometry* **2006**, 20, (18), 2747-2752.

[77] Nagai, R.; Unno, Y.; Hayashi, M. C.; Masuda, S.; Hayase, F.; Kinae, N.; Horiuchi, S. Formation of Nε -(Carboxymethyl)Lysine by the Cleavage of Amadori Product and Generation of Glucosone and Glyoxal From Glucose Novel Pathways for Protein Modification by Peroxynitrite. *Diabetes* **2005**, 51, 2833-2839.

[78] Sang, S.; Shao, X.; Bai, N.; Lo, C.-Y.; Yang, C. S.; Ho, C.-T. Tea polyphenol (-)-epigallocatechin-3-gallate: a new trapping agent of reactive dicarbonyl species. *Chemical research in toxicology* **2007**, 20, (12), 1862-1870.

[79] Fang, X.; Qiu, F.; Yan, B.; Wang, H.; Mort, A. J.; Stark, R. E. NMR studies of molecular structure in fruit cuticle polyesters. *Phytochemistry* **2001**, 57, (6), 1035-1042.

[80] Tsao, R.; Yang, R.; Young, J. C.; Zhu, H. Polyphenolic profiles in eight apple cultivars using high-performance liquid chromatography. *Journal of agricultural and food chemistry* **2003**, 51,

(21), 6347-6353.

[81] Lommen, A.; Godejohann, M.; Venema, D. P.; Hollman, P. C.; Spraul, M. Application of directly coupled HPLC-NMR-MS to the identification and confirmation of quercetin glycosides and phloretin glycosides in apple peel. *Analytical chemistry* **2000**, 72, (8), 1793-1797.

[82] Lee, K. W.; Kim, Y. J.; Kim, D.-O.; Lee, H. J.; Lee, C. Y. Major phenolics in apple and their contribution to the total antioxidant capacity. *Journal of Agriculture and Food Chemistry* **2003**, 51, (22), 6516-6520.

[83] Crespy, V.; Aprikian, O.; Morand, C.; Besson, C.; Manach, C.; Demigne, C.; Remesy, C. Bioavailability of phloretin and phloridzin in rats. *Journal of Nutrition* **2001**, 131, (12), 3227-3230.

[84] Mennen, L. I.; Sapinho, D.; Ito, H.; Bertrais, S.; Galan, P.; Hercberg, S.; Scalbert, A. Urinary flavonoids and phenolic acids as biomarkers of intake for polyphenol-rich foods. *British Journal of Nutrition* **2006**, 96, 191-198.

[85] Murphy, W. A.; Lumsden, R. D. Phloretin inhibition of glucose transport by the tapeworm Hymenolepis diminuta: a kinetic analysis. *Comparative Biochemistry and Physiology Part A: Physiology* **1984**, 78, (4), 749-754.

[86] Minami, H.; Kim, J. R.; Tada, K.; Takahashi, F.; Miyamoto, K.; Nakabou, Y.; Sakai, K.; Hagihira, H. Inhibition of glucose absorption by phlorizin affects intestinal functions in rats. *Gastroenterology* **1993**, 105, (3), 692-697.

Curriculum Vitae

Xi Shao

EADUCATION

Rutgers University, New Brunswick, NJ
Ph.D. in Food Science, October 2010

M.S. in Food Science, June 2007

Capital Normal University, Beijing, China
B.S. in Chemistry, June 2005

ARTICLES PUBLISHED OR ACCEPTED

Naisheng Bai, Kan He, Marc Roller, Ching-Shu Lai, **Xi Shao**, Min-Hsiung Pan, Antoine Bily, Chi-Tang Ho. Flavonoid glycosides from *Microtea debilis* and their cytotoxic and anti-inflammatory effects. *Fitoterapia* (Accepted)

Naisheng Bai, Kan He, Zhu Zhou, Mei-Ling Tsai, Li Zhang, Zheng Quan, **Xi Shao**, Min-Hsiung Pan, Chi-Tang Ho. Flavonoids from Rabdosia rubescens exert anti-inflammatory and growth inhibitory effect against human leukemia HL-60 cells. *Food Chem.,* 2010, 122, 831-835.

Xi Shao, Xiaoxin Chen, Vladimir Badmaev, Chi-Tang Ho, Shengmin Sang, Structural identification of phase II metabolites of pterostilbene in mouse urine using liquid chromatography/ tandem mass spectrometry. *Rap. Commun. Mass Spectrom.*, 2010, 24, 1770-1778.

Naisheng Bai, Kan He, Marc Roller, Ching-Shu Lai, **Xi Shao**, Min-Hsiung Pan, Chi-Tang Ho, Flavonoids and Phenolic Compounds from *Rosmarinus officinalis*. *J. Agric. Food Chem.*, 2010, 58, 5363-5367.

LiShuang Lv, **Xi Shao**, Liyan Wang, Chi-Tang Ho, Shengmin Sang, Inhibition of Advanced glycation-end products through trapping effect of methylglyoxal by Stiblene glycoside from *Polygonum multiflorum* Thunb. *J. Agric. Food Chem.*, 2010, 58, 2239-2245.

Naisheng Bai, Kan He, Zhu Zhou, Mei-Ling Tsai, Li Zhang, Zheng Quan, **Xi Shao**, Min-Hsiung Pan, Chi-Tang Ho, *Ent*-Kaurane Diterpenoids from Rabdosia rubescens and Their Cytotoxic Effects on Human Cancer Cell Lines. *Planta Med.*, 2009, 75, 1–6.

Xi Shao, Naisheng Bai, Kan He, Chi-Tang Ho, Chung S. Yang, Shengmin Sang, Apple polyphenols, phloretin and phloridzin: new trapping agents of reactive dicarbonyl species. *Chem. Res. Toxicol.*, 2008, 21, 2042–2050.

Di Tan, Chih-Yu Lo, **Xi Shao**, Yu Wang, Shengmin Sang, Fereidoon Shahidi, Chi-Tang Ho, Trapping of Methylglyoxal by Tea Polyphenols, *Tea and tea Products: Health-promoting Properties*, Edited by Chi-Tang Ho, Jen-Kun Lin, Fereidoon Shahidi, CRC press, Taylor & Francis Group, 2008, 245-254.

Shengmin Sang**, Xi Shao**, Naisheng Bai, Chih-Yu Lo, Chung S. Yang, Chi-Tang Ho,Tea Polyphenol (−)-Epigallocatechin-3-Gallate: A New Trapping Agent of Reactive Dicarbonyl Species. *Chem. Res. Toxicol.,* 2007, 20, 1862–1870.